

Adinkra Height Yielding Matrix Numbers: Eigenvalue Equivalence Classes for Minimal Four-Color Adinkras

S. James Gates, Jr.^{1a}, Yangrui Hu^{2a}, and Kory Stiffler^{3a}

^a*Department of Physics, Brown University,
Box 1843, 182 Hope Street, Barus & Holley 545, Providence, RI 02912, USA*

ABSTRACT

An adinkra is a graph-theoretic representation of spacetime supersymmetry. Minimal four-color valise adinkras have been extensively studied due to their relations to minimal 4D, $\mathcal{N} = 1$ supermultiplets. Valise adinkras, although an important subclass, do not encode all the information present when a 4D supermultiplet is reduced to 1D. Eigenvalue equivalence classes for valise adinkra matrices exist, known as χ_o equivalence classes, where valise adinkras within the same χ_o equivalence class are isomorphic in the sense that adinkras within a χ_o -equivalence class can be transformed into each other via field redefinitions of the nodes. We extend this to non-valise adinkras, via Python code, providing a complete eigenvalue classification of “node-lifting” for all 36,864 valise adinkras associated with the Coxeter group BC_4 . We term the eigenvalues associated with these node-lifted adinkras Height Yielding Matrix Numbers (HYMNs) and introduce HYMN equivalence classes. These findings have been summarized in a *Mathematica* notebook that can found at the [HEPThools Data Repository](#) on GitHub.

PACS: 11.30.Pb, 12.60.Jv

Keywords: adinkra, isomorphism, supersymmetry

¹ sylvester_gates@brown.edu

² yangrui_hu@brown.edu

³ kory_stiffler@brown.edu

1 Introduction

The discovery of the role played by the $\mathcal{GR}(d,N)$ “Garden Algebras” [1,2] in the generation of representations of spacetime SUSY triggered the introduction of adinkras [3] in order to allow the technology of graph theory to include and expand prior existing results. Among these results was an algorithm for generating dimensions of the minimal linear representations for all possible supersymmetrical systems. This is encoded in a function denoted by $d_{min}(N)$ [1,2] where N is the number of one dimensional supercharges. In an adinkra graph, links denote the orbits of the one-dimensional projections of space-time functions in a supermultiplet under the action of space-time supercharges. The nodes of an adinkra graph are projections of the fields of a supermultiplet when their functional dependence is restricted to solely depend on time. Since their introduction, adinkras have also opened gateways to insights in the physics and mathematics of SUSY.

On the physics side, one of the most striking implications uncovered is every off-shell linear supersymmetrical system that allows for the solution of the initial value problem involves adinkras containing error-correcting codes [4,5,6]. This apparently implies an information-theoretic foundation is present in all supersymmetrical particle, field, and string theories.

On the mathematics side, in a correspondingly striking implication it is now known adinkras, due to the work of [7,8], may be regarded as examples of Grothendieck’s “dessin d’ enfant” and thereby define a class of Riemann surfaces. From this vantage point, the heights of the nodes in an adinkra correspond to an integer-valued discrete Morse function defined over these Riemann surfaces.

In 1970, the mathematician Banchoff [9]⁴ introduced a form of discrete Morse functions for oriented triangular meshes. For the case of the Riemann surfaces associated with adinkras, it is the value of the heights of the nodes (made into a piecewise-linear function over the meshes constructed by linear extension across the edges and faces of the plaquettes) that are used to define the Morse function. So the height assigned to each node may also be called the “Banchoff index” of the node.

Within 4D theories generally not all of the bosonic fields contained within a supermultiplet possess the same engineering dimensions. In a similar manner, in the general case, not all fermionic fields contained in a supermultiplet possess the same engineering dimensions. At the level of adinkra graphs, the engineering dimension of a particular projection of a space-time field determines the literal height at which the node representing that projection appears in the graphs. Fields with the lowest engineering dimension appear at the lowest level of an adinkra graph. Fields of higher engineering dimension appear at higher levels in the graph.

A special class of adinkras are those in which all the bosonic nodes in the adinkra appear at the same height and all the fermionic nodes in the adinkra have the same height (but which is different from the bosonic node height). These are called “valise” adinkras. In terms of the field theories of which such adinkras are their projections, all bosonic fields in the supermultiplet possess the same engineering dimension. A similar statement can be made about the fermionic fields of the supermultiplet.

Even before the introduction of adinkras, the phenomenon of “node lifting” and “node lowering” had been noticed [10]. The effect of lifting nodes in adinkra graphs was investigated in [11,12,14,15,16,13,17]. Using a Python program, we have computed eigenvalues of “B-matrices” of all sixteen adinkras corresponding to lifting bosonic nodes of each of the 36,864 $\mathcal{GR}(4,4)$ valise adinkra associated with the Coexter Group BC_4 . We refer to the eigenvalues of these B-matrices as Height Yielding Matrix Numbers (HYMNs). The main results of this paper are given in section 5 where we classify the B-matrices and

⁴The publications in [7,8] pointed toward the relevance of this work.

their associated node-raised adinkras in terms of HYMN equivalence classes. We find that the HYMN equivalence classes for valise adinkras are simply the χ_o -equivalence classes originally investigated in [18] and more formally defined in the recent work [19]. We find a bosonic node-lifting mirror symmetry in the HYMN equivalence classes for adinkras with two bosonic nodes raised. Source code in the Python language is provided in appendix B. A summary of the calculations can be found in a *Mathematica* notebook available at the HEPThools [Data Repository](#) on GitHub.

2 Review of 36,864 Four-Color Valise Adinkras

First, we will briefly review L-matrices. Here we use the 4D, $\mathcal{N} = 1$ chiral multiplet as an example. We have in our conventions for 4D quantities,

$$\begin{aligned} D_a A &= \psi_a \quad , \quad D_a B = i(\gamma^5)_a{}^b \psi_b \quad , \quad D_a F = (\gamma^\mu)_a{}^b \partial_\mu \psi_b \quad , \quad D_a G = i(\gamma^5 \gamma^\mu)_a{}^b \partial_\mu \psi_b \quad , \\ D_a \psi_b &= i(\gamma^\mu)_{ab} \partial_\mu A - (\gamma^5 \gamma^\mu)_{ab} \partial_\mu B - iC_{ab} F + (\gamma^5)_{ab} G \quad . \end{aligned} \quad (2.1)$$

These equations are still valid if we restrict the functions only to be dependent on the t -coordinate. Under this restriction, we get the 4D, $\mathcal{N} = 1$ chiral multiplet on the 0-Brane. Define

$$\begin{aligned} \psi_1 &= i\Psi_1 \quad , \quad \psi_2 = i\Psi_2 \quad , \quad \psi_3 = i\Psi_3 \quad , \quad \psi_4 = i\Psi_4 \quad , \\ \Phi_1 &= A \quad , \quad \Phi_2 = B \quad , \quad \partial_0 \Phi_3 = F \quad , \quad \partial_0 \Phi_4 = G \quad , \end{aligned} \quad (2.2)$$

and rewrite (2.1) on the 0-Brane in the form

$$D_I \Phi_i = i(L_I)_{i\hat{k}} \Psi_{\hat{k}} \quad , \quad (2.3a)$$

$$D_I \Psi_{\hat{k}} = (R_I)_{\hat{k}i} \frac{d}{dt} \Phi_i \quad , \quad (2.3b)$$

where $I = 1, 2, 3, 4$ is the color index.

Note that in (2.2) the projections of the 4D fields A and B are directly related to adinkra nodal functions according to $\Phi_1 = A$, $\Phi_2 = B$, while the projections of the 4D fields F and G are related to adinkra nodal functions according to $\partial_0 \Phi_3 = F$, $\partial_0 \Phi_4 = G$. That is the adinkra nodal functions Φ_3 and Φ_4 are the integrals of the projections of the 4D fields F and G . Whenever an integral is used to define an adinkra node starting from the projection of a 4D field, we refer to this process as “nodal lowering.” This concept was first presented in the work of [10].

Consequently, we derive the explicit form of L-matrices:

$$\begin{aligned} (L_1)_{i\hat{k}} &= \begin{pmatrix} 1 & 0 & 0 & 0 \\ 0 & 0 & 0 & -1 \\ 0 & 1 & 0 & 0 \\ 0 & 0 & -1 & 0 \end{pmatrix} \quad , \quad (L_2)_{i\hat{k}} = \begin{pmatrix} 0 & 1 & 0 & 0 \\ 0 & 0 & 1 & 0 \\ -1 & 0 & 0 & 0 \\ 0 & 0 & 0 & -1 \end{pmatrix} \quad , \\ (L_3)_{i\hat{k}} &= \begin{pmatrix} 0 & 0 & 1 & 0 \\ 0 & -1 & 0 & 0 \\ 0 & 0 & 0 & -1 \\ 1 & 0 & 0 & 0 \end{pmatrix} \quad , \quad (L_4)_{i\hat{k}} = \begin{pmatrix} 0 & 0 & 0 & 1 \\ 1 & 0 & 0 & 0 \\ 0 & 0 & 1 & 0 \\ 0 & 1 & 0 & 0 \end{pmatrix} \quad . \end{aligned} \quad (2.4)$$

The R-matrices can be obtained by the relation $(R_I) = [(L_I)]^T$, where T superscript means transposition. The general algebra for $d \times d$ matrices describing N supersymmetries, known as the $\mathcal{GR}(d, N)$

algebra (garden algebra) is

$$\begin{aligned} (L_I)_{i\hat{k}}(R_J)_{\hat{k}j} + (L_J)_{i\hat{k}}(R_I)_{\hat{k}j} &= 2\delta_{IJ}\delta_{ij} \quad , \\ (R_I)_{i\hat{k}}(L_J)_{\hat{k}j} + (R_J)_{i\hat{k}}(L_I)_{\hat{k}j} &= 2\delta_{IJ}\delta_{\hat{i}\hat{j}} \quad . \end{aligned} \quad (2.5)$$

The $(L_I)_{i\hat{k}}$ and $(R_I)_{\hat{k}i}$ matrices described by Eqs. (2.4) satisfy the $\mathcal{GR}(4,4)$ algebra.

The adinkra diagram for the off-shell chiral multiplet where the associated L-matrices appear in Eq. (2.4) is shown as Figure 1, where D₁-green, D₂-violet, D₃-orange, D₄-red.

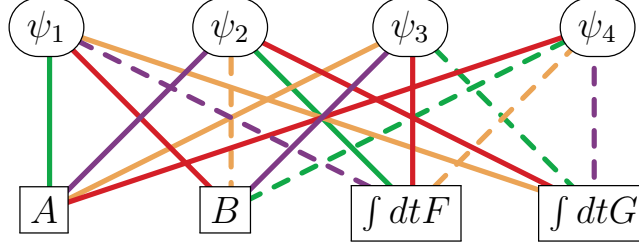


Figure 1: Valise Adinkra for Chiral Supermultiplet with F & G Nodes Lowered

Next, we will briefly introduce an algorithm to obtain all four-color valise adinkras. The recent work [19] studied how to generate all 36,864 four-color valise adinkras from only two basis valise adinkras given the titles of “quaternion adinkras.”

By definition, BC_4 is the group of signed permutations of four elements. BC_4 can be expressed as plus or minus one times a sign flip element times a permutation element times an element of the Vierergruppe.

$$BC_4^{\pm a\mu A} = \pm H^a S_3^\mu \mathcal{V}^A, \quad (2.6)$$

where H^a is a sign flip element and $a = 1, 2, \dots, 8$

$$H^a = \{(), (\overline{12}), (\overline{13}), (\overline{23}), (\overline{1}), (\overline{2}), (\overline{3}), (\overline{123})\}, \quad (2.7)$$

S_3^μ is a permutation element and $\mu = 1, 2, \dots, 6$

$$S_3^\mu = \{(), (12), (13), (23), (123), (132)\}, \quad (2.8)$$

\mathcal{V}^A is an element of the Vierergruppe and $A = 1, 2, 3, 4$

$$\mathcal{V}^A = \{(), (12)(34), (13)(24), (14)(23)\}. \quad (2.9)$$

The explicit matrix forms for these elements are given in [19]. As in [19], we refer to sign flips such as H^a as simply *flips* and permutations such as $S_3^\mu \mathcal{V}^A$ as *flops*.

All four-color valise adinkras can be generated by combinations of transformations.

$$\begin{aligned} (L_I^{\pm a\mu Ab\nu})_{i\hat{j}} &= (BC_4^{\pm a\mu A})_{i\hat{j}} (H^b S_3^\nu)_I^J (L_J^{(Q)})_{j\hat{j}}, \\ (\tilde{L}_I^{\pm a\mu Ab\nu})_{i\hat{j}} &= (BC_4^{\pm a\mu A})_{i\hat{j}} (H^b S_3^\nu)_I^J (\tilde{L}_J^{(\tilde{Q})})_{j\hat{j}}. \end{aligned} \quad (2.10)$$

where $(L_J^{(Q)})_{j\hat{j}}$ and $(\tilde{L}_J^{(\tilde{Q})})_{j\hat{j}}$ denote the L-matrices associated with the quaternionic basis adinkras to be given shortly.

index	\pm	a	μ	A	b	ν	\sim
count	2	8	6	4	8	6	2

The counting is summarized as the following table. The total product is 36,864. Thus, there are totally 36,864 four-color valise adinkras.

We define BC_4 color transformations as $(BC_4^{\pm a\mu A})_I^J$, where I, J are the color indices; BC_4 boson transformations as $(BC_4^{\pm a\mu A})_i^j$, where i, j are the bosonic indices; BC_4 fermion transformations as $(BC_4^{\pm a\mu A})_{\hat{i}}^{\hat{j}}$, where \hat{i}, \hat{j} are the fermionic indices. The definitions of the L-matrices associated with the quaternion basis adinkras Q and \tilde{Q} take the explicit forms,

$$\begin{aligned}
L_1^{(Q)} &= \begin{pmatrix} 1 & 0 & 0 & 0 \\ 0 & 1 & 0 & 0 \\ 0 & 0 & 1 & 0 \\ 0 & 0 & 0 & 1 \end{pmatrix}, & L_2^{(Q)} &= \begin{pmatrix} 0 & -1 & 0 & 0 \\ 1 & 0 & 0 & 0 \\ 0 & 0 & 0 & -1 \\ 0 & 0 & 1 & 0 \end{pmatrix}, \\
L_3^{(Q)} &= \begin{pmatrix} 0 & 0 & -1 & 0 \\ 0 & 0 & 0 & 1 \\ 1 & 0 & 0 & 0 \\ 0 & -1 & 0 & 0 \end{pmatrix}, & L_4^{(Q)} &= \begin{pmatrix} 0 & 0 & 0 & -1 \\ 0 & 0 & -1 & 0 \\ 0 & 1 & 0 & 0 \\ 1 & 0 & 0 & 0 \end{pmatrix}, \\
L_1^{(\tilde{Q})} &= \begin{pmatrix} 1 & 0 & 0 & 0 \\ 0 & 1 & 0 & 0 \\ 0 & 0 & 1 & 0 \\ 0 & 0 & 0 & 1 \end{pmatrix}, & L_2^{(\tilde{Q})} &= \begin{pmatrix} 0 & 1 & 0 & 0 \\ -1 & 0 & 0 & 0 \\ 0 & 0 & 0 & -1 \\ 0 & 0 & 1 & 0 \end{pmatrix}, \\
L_3^{(\tilde{Q})} &= \begin{pmatrix} 0 & 0 & -1 & 0 \\ 0 & 0 & 0 & -1 \\ 1 & 0 & 0 & 0 \\ 0 & 1 & 0 & 0 \end{pmatrix}, & L_4^{(\tilde{Q})} &= \begin{pmatrix} 0 & 0 & 0 & -1 \\ 0 & 0 & 1 & 0 \\ 0 & -1 & 0 & 0 \\ 1 & 0 & 0 & 0 \end{pmatrix}.
\end{aligned} \tag{2.11}$$

Since the early 1980's [20] and in later work (see for example [21,22,23,24]) it has been understood that division algebras play a significant role in the representations of spacetime SUSY. The results in (2.11) situate these previous observations in the context of $\mathcal{GR}(d, N)$ algebras. In fact the embedding of the quaternions realized by the matrices in (2.11) also matches the initial presentation on $\mathcal{GR}(d, N)$ algebras in [1,2]. The recursion formulae given in these earliest works on Garden Algebras also solve a puzzle.

The division algebras only exists up to the octonions. This is equivalent to 4D, $\mathcal{N} = 2$ spacetime SUSY. Since realizations of SUSY exist beyond 4D, $\mathcal{N} = 2$, the puzzle was to ask, "What replaces the division algebras for the higher theories?" In the works of [1,2] such extensions were created for all values of \mathcal{N} using a recursion formula that realizes Bott periodicity as reviewed in appendix A.

3 Adinkra Height Related 4D, $\mathcal{N} = 1$ Minimal Supermultiplets

The chiral supermultiplet is only one member of a group of ten such supermultiplets that lead to adinkras of the same general form as that shown in Fig. 1.

There are three versions of the 4D, $\mathcal{N} = 1$ chiral supermultiplet related to the standard version discussed above by Hodge duality transformation applied to the auxiliary fields. These take the forms shown in equations (3.1), (3.2), and (3.3), respectively.

Hodge – Dual #1 Chiral Supermultiplet : $(A, B, \psi_a, f_{\mu\nu\rho}, G)$

$$\begin{aligned}
D_a A &= \psi_a \quad , \quad D_a B = i(\gamma^5)_a{}^b \psi_b \quad , \\
D_a \psi_b &= i(\gamma^\mu)_{ab} \partial_\mu A - (\gamma^5 \gamma^\mu)_{ab} \partial_\mu B - i \frac{1}{3!} C_{ab} (\epsilon^{\sigma\mu\nu\rho} \partial_\sigma f_{\mu\nu\rho}) + (\gamma^5)_{ab} G \quad , \\
D_a f_{\mu\nu\rho} &= -(\gamma^\sigma)_a{}^b \epsilon_{\sigma\mu\nu\rho} \psi_b \quad , \quad D_a G = i(\gamma^5 \gamma^\mu)_a{}^b \partial_\mu \psi_b \quad ,
\end{aligned} \tag{3.1}$$

Hodge – Dual #2 Chiral Supermultiplet : $(A, B, \psi_a, F, g_{\mu\nu\rho})$

$$\begin{aligned}
D_a A &= \psi_a \quad , \quad D_a B = i(\gamma^5)_a{}^b \psi_b \quad , \\
D_a \psi_b &= i(\gamma^\mu)_{ab} \partial_\mu A - (\gamma^5 \gamma^\mu)_{ab} \partial_\mu B - i C_{ab} F + \frac{1}{3!} (\gamma^5)_{ab} (\epsilon^{\sigma\mu\nu\rho} \partial_\sigma g_{\mu\nu\rho}) \quad , \\
D_a F &= (\gamma^\mu)_a{}^b \partial_\mu \psi_b \quad , \quad D_a g_{\mu\nu\rho} = -(\gamma^5 \gamma^\sigma)_a{}^b \epsilon_{\sigma\mu\nu\rho} \psi_b \quad ,
\end{aligned} \tag{3.2}$$

Hodge – Dual #3 Chiral Supermultiplet : $(A, B, \psi_a, f_{\mu\nu\rho}, g_{\mu\nu\rho})$

$$\begin{aligned}
D_a A &= \psi_a \quad , \quad D_a B = i(\gamma^5)_a{}^b \psi_b \quad , \\
D_a \psi_b &= i(\gamma^\mu)_{ab} \partial_\mu A - (\gamma^5 \gamma^\mu)_{ab} \partial_\mu B \\
&\quad - i \frac{1}{3!} C_{ab} (\epsilon^{\sigma\mu\nu\rho} \partial_\sigma f_{\mu\nu\rho}) + \frac{1}{3!} (\gamma^5)_{ab} (\epsilon^{\sigma\mu\nu\rho} \partial_\sigma g_{\mu\nu\rho}) \quad , \\
D_a f_{\mu\nu\rho} &= -(\gamma^\sigma)_a{}^b \epsilon_{\sigma\mu\nu\rho} \psi_b \quad , \quad D_a g_{\mu\nu\rho} = -(\gamma^5 \gamma^\sigma)_a{}^b \epsilon_{\sigma\mu\nu\rho} \psi_b \quad .
\end{aligned} \tag{3.3}$$

The engineering dimensions of the three-form gauge fields that appear above are the same as those of the A and B fields. So in an adinkra without node lowering, these three-form fields appear at the same height as the A and B fields. This has implications for how the component fields in these supermultiplets are related to the graph shown in Fig. 1.

For the *Hodge – Dual #1 Chiral Supermultiplet* one should perform the replacement in Fig. 1. of the auxiliary fields according to

$$\int dt F \rightarrow f_{123} \quad , \quad G \rightarrow G \quad , \tag{3.4}$$

where f_{123} is the purely spatial component of the Lorentz 3-form $f_{\mu\nu\rho}$.

For the *Hodge – Dual #2 Chiral Supermultiplet* one should perform the replacement in Fig. 1. of the auxiliary fields according to

$$F \rightarrow F \quad , \quad \int dt G \rightarrow g_{123} \quad , \tag{3.5}$$

where g_{123} is the purely spatial component of the Lorentz 3-form $g_{\mu\nu\rho}$.

For the *Hodge – Dual #3 Chiral Supermultiplet* one should perform the replacement in Fig. 1 of the auxiliary fields according to

$$\int dt F \rightarrow f_{123} \quad , \quad \int dt G \rightarrow g_{123} \quad , \tag{3.6}$$

where f_{123} is the purely spatial component of the Lorentz 3-form $f_{\mu\nu\rho}$ and g_{123} is the purely spatial component of the Lorentz 3-form $g_{\mu\nu\rho}$.

The parity transformations and Hodge dual transformations carried out on the standard chiral supermultiplet can be extended to vector supermultiplets as well. This leads to the supermultiplets described

by the four equations seen in (3.7) - (3.10) according to:

Vector Supermultiplet : (A_μ, λ_b, d)

$$\begin{aligned} D_a A_\mu &= (\gamma_\mu)_a{}^b \lambda_b \quad , \\ D_a \lambda_b &= -i \frac{1}{4} ([\gamma^\mu, \gamma^\nu])_{ab} (\partial_\mu A_\nu - \partial_\nu A_\mu) + (\gamma^5)_{ab} d \quad , \\ D_a d &= i (\gamma^5 \gamma^\mu)_a{}^b \partial_\mu \lambda_b \quad , \end{aligned} \tag{3.7}$$

Axial – Vector Supermultiplet : $(U_\mu, \tilde{\lambda}_b, \tilde{d})$

$$\begin{aligned} D_a U_\mu &= i (\gamma^5 \gamma_\mu)_a{}^b \tilde{\lambda}_b \quad , \\ D_a \tilde{\lambda}_b &= \frac{1}{4} (\gamma^5 [\gamma^\mu, \gamma^\nu])_{ab} (\partial_\mu U_\nu - \partial_\nu U_\mu) + i C_{ab} \tilde{d} \quad , \\ D_a \tilde{d} &= -(\gamma^\mu)_a{}^b \partial_\mu \tilde{\lambda}_b \quad , \end{aligned} \tag{3.8}$$

Hodge – Dual Vector Supermultiplet : $(A_\mu, \lambda_b, d_{\mu\nu\rho})$

$$\begin{aligned} D_a A_\mu &= (\gamma_\mu)_a{}^b \lambda_b \quad , \\ D_a \lambda_b &= -i \frac{1}{4} ([\gamma^\mu, \gamma^\nu])_{ab} (\partial_\mu A_\nu - \partial_\nu A_\mu) + \frac{1}{3!} (\gamma^5)_{ab} (\epsilon^{\sigma\mu\nu\rho} \partial_\sigma d_{\mu\nu\rho}) \quad , \\ D_a d &= i (\gamma^5 \gamma^\mu)_a{}^b \partial_\mu \lambda_b \quad , \end{aligned} \tag{3.9}$$

Hodge – Dual Axial – Vector Supermultiplet : $(A_\mu, \tilde{\lambda}_b, \tilde{d}_{\mu\nu\rho})$

$$\begin{aligned} D_a U_\mu &= i (\gamma^5 \gamma_\mu)_a{}^b \tilde{\lambda}_b \quad , \\ D_a \tilde{\lambda}_b &= \frac{1}{4} (\gamma^5 [\gamma^\mu, \gamma^\nu])_{ab} (\partial_\mu U_\nu - \partial_\nu U_\mu) + i \frac{1}{3!} C_{ab} (\epsilon^{\sigma\mu\nu\rho} \partial_\sigma \tilde{d}_{\mu\nu\rho}) \quad , \\ D_a \tilde{d} &= -(\gamma^\mu)_a{}^b \partial_\mu \tilde{\lambda}_b \quad , \end{aligned} \tag{3.10}$$

One can continue by applying Hodge transformations to the propagating physical bosons of the chiral supermultiplet. There are theories associated with performing the duality on either the scalar or pseudoscalar in the supermultiplet. In the former case this leads to the tensor supermultiplet shown in (3.11), while in the latter case the duality transformation leads to the axial-tensor supermultiplet shown in (3.12).

Tensor Supermultiplet : $(\varphi, B_{\mu\nu}, \chi_a)$

$$\begin{aligned} D_a \varphi &= \chi_a \quad , \quad D_a B_{\mu\nu} = -\frac{1}{4} ([\gamma_\mu, \gamma_\nu])_a{}^b \chi_b \quad , \\ D_a \chi_b &= i (\gamma^\mu)_{ab} \partial_\mu \varphi - (\gamma^5 \gamma^\mu)_{ab} \epsilon_\mu{}^{\rho\sigma\tau} \partial_\rho B_{\sigma\tau} \quad , \end{aligned} \tag{3.11}$$

Axial – Tensor Supermultiplet : $(\tilde{\varphi}, C_{\mu\nu}, \tilde{\chi}_a)$

$$\begin{aligned} D_a \tilde{\varphi} &= -i (\gamma^\mu)_a{}^b \tilde{\chi}_b \quad , \quad D_a C_{\mu\nu} = -i \frac{1}{4} (\gamma^5 [\gamma_\mu, \gamma_\nu])_a{}^b \tilde{\chi}_b \quad , \\ D_a \tilde{\chi}_b &= -(\gamma^5 \gamma^\mu)_{ab} \partial_\mu \tilde{\varphi} - i (\gamma^\mu)_{ab} \epsilon_\mu{}^{\rho\sigma\tau} \partial_\rho C_{\sigma\tau} \quad , \end{aligned} \tag{3.12}$$

From these results, it is seen there are no explicit auxiliary fields in either case. Implicitly, such fields are present in the gauge two-forms contained in each supermultiplet.

One might be tempted to continue the process of performing a Hodge duality on the remaining scalar or pseudoscalar in either of the two version of a tensor supermultiplet above. This was carried out in

a little known work [25] by Freedman many years ago. However, the field theory that results from this “dualization” is distinguished from all the other supermultiplets described in the chapter. Namely, one can use the transformation laws of the ten supermultiplets given in (2.1), (3.1), . . . , (3.12) to show the condition

$$\{D_a, D_b\} = i2(\gamma^\mu)_{ab}\partial_\mu \quad (3.13)$$

is satisfied (up to gauge transformations) on every component field...except in the case where Hodge dualization is carried on scalar and pseudoscalar in the two tensor supermultiplets above.

So all toll, there are ten minimal *off-shell* 4D, $\mathcal{N} = 1$ supermultiplets.

4 HYMNs: Height Yielding Matrix Numbers

Valise adinkras have the advantage of being the simplest type of adinkra. However, we know that when attempting to use adinkra-based arguments to re-construct higher dimensional field theory representations, the simplicity of valise adinkras interacts with the requirement of the realization of Lorentz symmetry in the higher dimensions [14,15,16]. There can arise obstructions as pointedly noted in [16,17] where the conditions for selecting which adinkras can be used as a basis for the re-construction of 2D world sheet supersymmetric theories. These works demonstrate that the shape of a non-valise adinkra is an important attribute to knowing what higher dimensional physics relates to which adinkra systems.

In the works of [11,12,13] two apparently distinct approaches were presented as a way to characterize the shape of non-valise adinkras. In particular, the second of these approaches in [13] makes explicit the appearance of a particular matrices derived from the L-matrices and R-matrices. These derived matrices can be called the “left B-matrix” and the “right B-matrix.” Due to their relations to the work in [9] this is a highly appropriate name. The eigenvalues of the B-matrices relate to the shape of all adinkras including therefore, non-valise ones. In the following discussion we are going to define the B-matrices in a manner that is slightly different from the work [13]. Our new method has the benefit of categorizing raised-node adinkras in a way that is manifestly color-independent, or supersymmetric charge-independent, in contrast to the methods of [13] which are manifestly color-dependent.

In the work of [13] a proposition was made for when two adinkras are isomorphic that involved the two matrices constructed similarly to $B_L = L_N R_{N-1} L_{N-2} \cdots$ and $B_R = R_N L_{N-1} R_{N-2} \cdots$ that contained color-dependent height parameters β_I . It was proposed that if two adinkras are isomorphic, their chromocharacters and their eigenvalues for B_L and B_R are the same. The chromocharacter of a non-valise adinkra is defined, up to a normalization, as the trace of its B_L matrix after setting all β_I to one. This indicates an importance in developing eigenvalue equivalence classes for non-valise adinkras, which we wish to do in color-independent way without use of the β_I . We have recently developed a new procedure to define such eigenvalue equivalence classes. In this section, we will briefly describe this procedure using the simplest non-trivial adinkras. We begin by revisiting the valise adinkra for the chiral multiplet, where we notice the mass dimensions of the fields are:

$$[\Phi_i] = 1 \quad , \quad [\Psi_{\dot{i}}] = 3/2 \quad . \quad (4.1)$$

For any valise adinkra, the bosons will all have the same mass dimension and the fermions will all have the same mass dimension that is one-half higher than the bosons. We can raise the nodes associated with the auxiliary bosons F and G via the raising operator M , defined below along with its inverse, the lowering

operator M^{-1}

$$M = \begin{pmatrix} 1 & 0 & 0 & 0 \\ 0 & 1 & 0 & 0 \\ 0 & 0 & \partial_0 & 0 \\ 0 & 0 & 0 & \partial_0 \end{pmatrix} , \quad M^{-1} = \begin{pmatrix} 1 & 0 & 0 & 0 \\ 0 & 1 & 0 & 0 \\ 0 & 0 & \int dt & 0 \\ 0 & 0 & 0 & \int dt \end{pmatrix} . \quad (4.2)$$

The M operator raises nodes by performing the field redefinition:

$$\tilde{\Phi} = M\Phi = \begin{pmatrix} A \\ B \\ F \\ G \end{pmatrix} . \quad (4.3)$$

This results in the following mass dimensions for the tilded fields $\tilde{\Phi}_i$:

$$[\tilde{\Phi}_1] = [\tilde{\Phi}_2] = 1 \quad , \quad [\tilde{\Phi}_3] = [\tilde{\Phi}_4] = 2 \quad . \quad (4.4)$$

Operating on Eq. (2.3a) from the left with M results in the following:

$$\begin{aligned} D_I M\Phi &= i M L_I \Psi \quad , \\ D_I \tilde{\Phi} &= i \tilde{L}_I \tilde{\Psi} \quad , \end{aligned} \quad (4.5)$$

where we have defined $\tilde{\Psi} = \Psi$ and \tilde{L}_I as follows

$$\tilde{L}_I = M L_I \quad . \quad (4.6)$$

Inserting $M^{-1}M = I$ into Eq. (2.3b) results in

$$\begin{aligned} D_I \Psi &= R_I M^{-1} M\Phi \quad , \\ D_I \tilde{\Psi} &= \tilde{R}_I \tilde{\Phi} \quad . \end{aligned} \quad (4.7)$$

We write the results in Eqs. (4.5) and (4.7) succinctly as the transformation laws for $\tilde{\Phi}$ and $\tilde{\Psi}$:

$$D_I \tilde{\Phi} = i \tilde{L}_I \tilde{\Psi} \quad , \quad (4.8a)$$

$$D_I \tilde{\Psi} = \tilde{R}_I \tilde{\Phi} \quad . \quad (4.8b)$$

It is straightforward to show that \tilde{L}_I and \tilde{R}_I satisfy the garden algebra, Eq. (2.5), written instead in terms of these tilded matrices. The adinkra matrices \tilde{L}_I and \tilde{R}_I now have height information, in the derivatives and integrals, and can be expressed as the three-level adinkra in Fig. 2

To investigate such node liftings of adinkras, it will be advantageous to forget the integral/derivative nature of lowering/raising nodes and instead simply use mass parameters to keep track the lowered/raised nodes. We make the substitution

$$\partial_0 F \rightarrow mF \quad , \quad \partial_0 G \rightarrow mG \quad . \quad (4.9)$$

For instance, for the chiral multiplet M and its inverse could have been defined instead as

$$M(m) = \begin{pmatrix} 1 & 0 & 0 & 0 \\ 0 & 1 & 0 & 0 \\ 0 & 0 & m & 0 \\ 0 & 0 & 0 & m \end{pmatrix} , \quad (4.10)$$

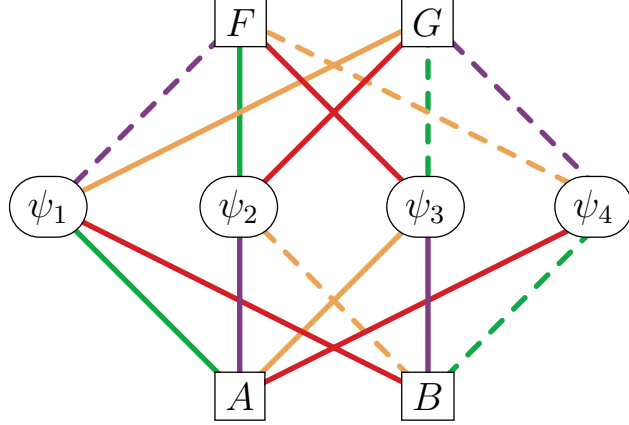


Figure 2: Adinkra for Chiral Supermultiplet without F & G Nodes Lowered

and Eqs. (4.5) through (4.8) would have followed the same as before.

Next, we generalize these node raising matrices to arbitrarily sized $d \times d$ adinkras. The $\mathcal{GR}(d, N)$ SUSY transformation laws are

$$D_I \Phi = i L_I \Psi \quad , \quad (4.11)$$

$$D_I \Psi = R_I \dot{\Phi} \quad , \quad (4.12)$$

where a dot above a field indicates a time derivative: $\dot{\Phi} = d\Phi/dt$. The L_I and R_I matrices realize the closed $N = 4$ SUSY algebra for d bosons and d fermions as the $\mathcal{GR}(d, N)$ algebra

$$L_I R_J + L_J R_I = 2\delta_{IJ} I_{d \times d} \quad , \quad (4.13)$$

$$R_I L_J + R_J L_I = 2\delta_{IJ} I_{d \times d} \quad , \quad (4.14)$$

with $I_{d \times d}$ the $d \times d$ identity matrix.

We define the node raising operator $M(m, w)$ that acts on an arbitrary number of d bosons as

$$M(m, w) \equiv \begin{pmatrix} m^{p_1} & 0 & 0 & \dots & 0 \\ 0 & m^{p_1} & 0 & \dots & 0 \\ 0 & 0 & m^{p_3} & \dots & 0 \\ \vdots & \vdots & \vdots & \ddots & 0 \\ 0 & 0 & 0 & \dots & m^{p_d} \end{pmatrix} \quad , \quad (4.15)$$

$$w \equiv p_1 2^0 + p_2 2^1 + p_3 2^2 + \dots + p_d 2^{d-1} \quad , \quad \text{with } p_i = 0, 1 \quad (4.16)$$

where the word parameter w is as in [29]. The node raising operator $M(m, w)$ has the following combination properties

$$M(1, w) = I_{d \times d} \quad , \quad (4.17)$$

$$M(m, w) M(\mu, w) = M(m\mu, w) \quad , \quad (4.18)$$

$$M(m, w_1) M(m, w_2) = M(m, w_1 + w_2) \quad , \quad (4.19)$$

$$[M(m, w)]^{-1} = M(m^{-1}, w) \quad , \quad (4.20)$$

$$M(m, w)[M(\mu, w)]^{-1} = M(m/\mu, w) \quad , \quad (4.21)$$

We denote a raised node boson collection as $\Phi(m, w)$

$$\Phi(m, w) = M(m, w)\Phi \quad . \quad (4.22)$$

Multiplying Eq. (4.11) from the left by $M(m, w)$ and inserting $I_{d \times d} = M(\mu, w)[M(\mu, w)]^{-1}$ into the right hand side of Eq. (4.12) results in

$$\begin{aligned} D_I M(m, w)\Phi &= iM(m, w)L_I\Psi \quad , \\ D_I\Psi &= R_I[M(\mu, w)]^{-1}M(\mu, w)\dot{\Phi} = R_I M(\mu^{-1}, w)M(\mu, w)\dot{\Phi} \quad , \end{aligned} \quad (4.23)$$

We now make the matrix redefinitions

$$L_I(m, w) = M(m, w)L_I \quad , \quad R_I(\mu, w) = R_I M(\mu^{-1}, w) \quad (4.24)$$

which along with the field redefinitions in Eq. (4.22) reduces Eqs. (4.23) to

$$D_I\Phi(m, w) = iL_I(m, w)\Psi \quad , \quad D_I\Psi = R_I(\mu, w)\dot{\Phi}(\mu, w) \quad (4.25)$$

It is important to make clear the meaning of the matrices $L_I(m, w)$ and $R_I(\mu, w)$ as these are the "deformed" version of the L_I and R_I for adinkras where the some number of bosonic and fermionic nodes have been lifted from the corresponding level in a valise adinkra within the context of BC_4 related adinkras. It will be necessary to modify our formalism in the future to handle the cases where nodes can be lifted to a height that is greater than one about that which the node appears in a corresponding valise adinkra.

The redefined matrices $L_I(m, w)$ and $R_I(\mu, w)$ satisfy the $GR(d, N)$ algebra in the $\mu \rightarrow m$ limit:

$$\begin{aligned} L_I(m, w)R_J(\mu, w) + L_J(m, w)R_I(\mu, w) &= M(m, w)(L_I R_J + L_J R_I)M(\mu^{-1}, w) \\ &= 2\delta_{IJ}M(m, w)M(\mu^{-1}, w) \\ &= 2\delta_{IJ}M(m/\mu, w) \\ &\rightarrow 2\delta_{IJ}I_{d \times d} \quad , \quad \text{for } \mu \rightarrow m \end{aligned} \quad (4.26)$$

where going from the second to third line we have made use of the property in Eq. (4.18) and in going from the third to last line have made use of the property in Eq. (4.21). The same results holds in the $\mu \rightarrow m$ limit for the $R_I L_J + R_J L_I$ algebra in Eq. (4.14), though the details are different:

$$\begin{aligned} R_I(\mu, w)L_J(m, w) + R_J(\mu, w)L_I(m, w) &= R_I M(\mu^{-1}, w)M(m, w)L_J + R_J M(\mu^{-1}, w)M(m, w)L_I \\ &= R_I M(m/\mu, w)L_J + R_J M(m/\mu, w)L_I \\ &\rightarrow R_I L_J + R_J L_I = 2\delta_{IJ}I_{d \times d} \quad , \text{for } \mu \rightarrow m \quad . \end{aligned} \quad (4.27)$$

In order to describe adinkras uniquely, the color dependent block matrix C_I associated with the I -th color is defined as

$$C_I = \begin{pmatrix} 0 & L_I \\ R_I & 0 \end{pmatrix} \quad . \quad (4.28)$$

Since every path can be covered by looking at the N distinct color paths from a boson or fermion, we can define the B matrix by multiplying all of the color matrices

$$B = C_N C_{N-1} C_{N-2} \cdots C_1 \quad . \quad (4.29)$$

If N is odd,

$$B = \begin{pmatrix} 0 & L_N R_{N-1} \cdots L_1 \\ R_N L_{N-1} \cdots R_1 & 0 \end{pmatrix} \equiv \begin{pmatrix} 0 & B_L \\ B_R & 0 \end{pmatrix} , \quad (4.30)$$

and if N is even,

$$B = \begin{pmatrix} L_N R_{N-1} \cdots R_1 & 0 \\ 0 & R_N L_{N-1} \cdots L_1 \end{pmatrix} \equiv \begin{pmatrix} B_L & 0 \\ 0 & B_R \end{pmatrix} . \quad (4.31)$$

Any reader familiar with our work in [13] will recognize these definitions from that work. We here make the additional identification that the non-vanishing upper left hand entry in the last expression of (4.31) is what we mean by the left B- matrix and accordingly the non-vanishing lower right hand entry in the last expression of (4.31) is the right B-matrix. We define Height Yielding Matrix Numbers (HYMNs) as the eigenvalues of these matrices. It also is of note that in the case of odd values of N , the square of the matrix in (4.30) can be used to define the left and right B-matrices.

Permuting fermionic or bosonic nodes of a valise adinkra does not influence its HYMNs. We prove this in the following. We can assign that if we relabel fermionic nodes, the permutation matrix is P_F ; if we relabel bosonic nodes, the permutation matrix is P_B . Thus, after relabeling,

$$L_I \rightarrow P_B L_I P_F, \quad R_I \rightarrow P_F^T R_I P_B^T , \quad (4.32)$$

Consequently, when N is odd,

$$\begin{aligned} L_N R_{N-1} \cdots L_1 &\rightarrow P_B L_N P_F P_F^T R_{N-1} P_B^T \cdots P_B L_1 P_F = P_B (L_N R_{N-1} \cdots L_1) P_F , \\ R_N L_{N-1} \cdots R_1 &\rightarrow P_F^T R_N P_B^T P_B L_{N-1} P_F \cdots P_F^T R_1 P_B^T = P_F^T (R_N L_{N-1} \cdots R_1) P_B^T . \end{aligned} \quad (4.33)$$

When N is even,

$$\begin{aligned} L_N R_{N-1} \cdots R_1 &\rightarrow P_B L_N P_F P_F^T R_{N-1} P_B^T \cdots P_F^T R_1 P_B^T = P_B (L_N R_{N-1} \cdots R_1) P_B^T , \\ R_N L_{N-1} \cdots L_1 &\rightarrow P_F^T R_N P_B^T P_B L_{N-1} P_F \cdots P_B L_1 P_F = P_F^T (R_N L_{N-1} \cdots L_1) P_F . \end{aligned} \quad (4.34)$$

For all N , we can obtain

$$B \rightarrow \begin{pmatrix} P_B & 0 \\ 0 & P_F^T \end{pmatrix} B \begin{pmatrix} P_B^T & 0 \\ 0 & P_F \end{pmatrix} . \quad (4.35)$$

Thus, eigenvalues of B will not be changed after relabeling nodes, although eigenvalues of $L_N \dots L_1$ and $R_N \dots R_1$ may be changed when N is odd.

We conjecture that the HYMNs of an adinkra carry all information about its shape isomorphisms. Specifically, we conjecture that two adinkras are isomorphic if and only if their HYMNs are the same.

The parameter χ_o defines the two equivalence classes for $\mathcal{GR}(4, 4)$ valise adinkras with respect to signed permutations of bosonic and fermionic nodes [18]. The general definition of χ_o for adinkras with arbitrary number of colors N is [11,12]

$$\chi_o = \frac{1}{d_{\min}(N)} \frac{1}{N!} \epsilon^{I_1 I_2 \cdots I_N} \text{Tr}(L_{I_1} R_{I_2} \cdots L/R_{I_N}) , \quad (4.36)$$

where the last matrix in the trace will be L_{I_N} if N is odd and R_{I_N} if N is even. The quantity $d_{\min}(N)$ is a function of N first identified in the original works on Garden Algebras [1,2]

$$d_{\min}(N) = \begin{cases} 2^{\frac{N-1}{2}}, & N \equiv 1, 7 \pmod{8} \\ 2^{\frac{N}{2}}, & N \equiv 2, 4, 6 \pmod{8} \\ 2^{\frac{N+1}{2}}, & N \equiv 3, 5 \pmod{8} \\ 2^{\frac{N-2}{2}}, & N \equiv 8 \pmod{8} \end{cases} . \quad (4.37)$$

So far, the effect of lifting nodes on adinkra isomorphisms is generally unknown. In order to study this effect, we are developing a symbolic program of which we give examples in the following subsections.

4.1 Raised Boson Adinkras for $\mathcal{GR}(2, 2)$

Figure 3 shows one of the simplest two-color adinkras. The adinkra matrices for this adinkra are the following where L_1 -green and L_2 -purple:

$$\begin{aligned} L_1 &= \begin{pmatrix} 1 & 0 \\ 0 & 1 \end{pmatrix}, \quad R_1 = \begin{pmatrix} 1 & 0 \\ 0 & 1 \end{pmatrix}, \\ L_2 &= \begin{pmatrix} 0 & -1 \\ 1 & 0 \end{pmatrix}, \quad R_2 = \begin{pmatrix} 0 & 1 \\ -1 & 0 \end{pmatrix}. \end{aligned} \quad (4.38)$$

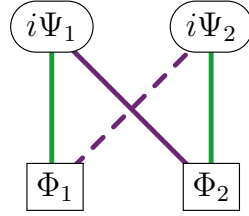


Figure 3: An example of a $\mathcal{GR}(2, 2)$ valise adinkra.

In Fig. 3 for instance, we can raise the first bosonic node with $M(m, 1)$, the second with $M(m, 2)$ and both with $M(m, 3) = M(m, 1)M(m, 2)$. These matrices and the corresponding raised boson collections $\Phi(m, w)$ are

$$\Phi(m, 1) = \begin{pmatrix} m\Phi_1 \\ \Phi_2 \end{pmatrix}, \quad M(m, 1) = \begin{pmatrix} m & 0 \\ 0 & 1 \end{pmatrix}, \quad (4.39a)$$

$$\Phi(m, 2) = \begin{pmatrix} \Phi_1 \\ m\Phi_2 \end{pmatrix}, \quad M(m, 2) = \begin{pmatrix} 1 & 0 \\ 0 & m \end{pmatrix}, \quad (4.39b)$$

$$\Phi(m, 3) = \begin{pmatrix} m\Phi_1 \\ m\Phi_2 \end{pmatrix}, \quad M(m, 3) = \begin{pmatrix} m & 0 \\ 0 & m \end{pmatrix}. \quad (4.39c)$$

The resulting adinkras for each of these three cases are given in Fig. 4.

According to Eq. (4.24), the adinkra matrices associated with Fig. 4 and nodal redefinitions in Eq. (4.39a) are as follows. The adinkra matrices corresponding to the leftmost adinkra in Fig. 4 with boson one raised are

$$\begin{aligned} L_1(m, 1) &= \begin{pmatrix} m & 0 \\ 0 & 1 \end{pmatrix}, \quad R_1(\mu, 1) = \begin{pmatrix} \mu^{-1} & 0 \\ 0 & 1 \end{pmatrix}, \\ L_2(m, 1) &= \begin{pmatrix} 0 & -m \\ 1 & 0 \end{pmatrix}, \quad R_2(\mu, 1) = \begin{pmatrix} 0 & 1 \\ -\mu^{-1} & 0 \end{pmatrix}. \end{aligned} \quad (4.40)$$

The adinkra matrices corresponding to the middle adinkra in Fig. 4 with boson two raised are

$$\begin{aligned} L_1(m, 2) &= \begin{pmatrix} 1 & 0 \\ 0 & m \end{pmatrix}, \quad R_1(\mu, 2) = \begin{pmatrix} 1 & 0 \\ 0 & \mu^{-1} \end{pmatrix}, \\ L_2(m, 2) &= \begin{pmatrix} 0 & -1 \\ m & 0 \end{pmatrix}, \quad R_2(\mu, 2) = \begin{pmatrix} 0 & \mu^{-1} \\ -1 & 0 \end{pmatrix}. \end{aligned} \quad (4.41)$$

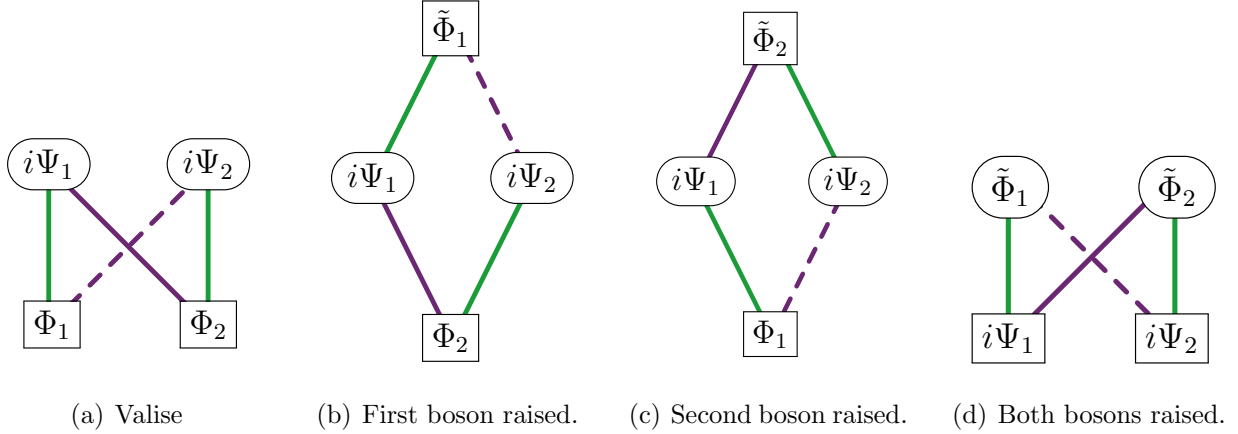


Figure 4: Valise and raised versions of the $\mathcal{GR}(2,2)$ adinkra of Fig. 3. The tilded bosons are identified as $\tilde{\Phi}_i = m\Phi_i$.

The adinkra matrices corresponding to the rightmost adinkra in Fig. 4 with both bosons raised are

$$\begin{aligned}
 L_1(m, 3) &= \begin{pmatrix} m & 0 \\ 0 & m \end{pmatrix}, & R_1(\mu, 3) &= \begin{pmatrix} \mu^{-1} & 0 \\ 0 & \mu^{-1} \end{pmatrix}, \\
 L_2(m, 3) &= \begin{pmatrix} 0 & -m \\ m & 0 \end{pmatrix}, & R_2(\mu, 3) &= \begin{pmatrix} 0 & \mu^{-1} \\ -\mu^{-1} & 0 \end{pmatrix}.
 \end{aligned} \tag{4.42}$$

The two color C_I matrix and B matrix given by Eqs. (4.28) and (4.31) are

$$C_I = \begin{pmatrix} 0 & L_I \\ R_I & 0 \end{pmatrix}, \quad B = C_2 C_1 = \begin{pmatrix} L_2 R_1 & 0 \\ 0 & R_2 L_1 \end{pmatrix}. \tag{4.43}$$

The eigenvalues of B are invariant with respect to fermionic and bosonic nodal transformations as described previously for the arbitrary N color case. With respect to color transformations, the eigenvalues of B are invariant with respect to even numbers of flips and flops, but odd numbers of flips and flops negate all eigenvalues. This is because of the $\mathcal{GR}(2,2)$ algebra relation $L_2 R_1 = -L_1 R_2$. The consequences of raising nodes are unknown as to the eigenvalues, so we next turn to the tabulation of all $\mathcal{GR}(2,2)$ adinkras, valise and raised.

The four images in Figure 4 illustrate a number of points in the abilities of adinkras to encode supermultiplet in higher dimensions. If these figures are interpreted to describe supermultiplets that solely depend on a single temporal coordinate, then we see there are three different types of supermultiplets.

The valise supermultiplet in Fig. 4(a) corresponds to the 1D projection of a 2D, $\mathcal{N} = (2,0)$ SUSY heterotic scalar supermultiplet [26,27] that resides on the world sheet of a string.

The two adinkras in Figs. 4(b) and 4(c) correspond to the 1D projection of a scalar supermultiplet on the world sheet of a string with (1,1) SUSY. In fact, these seemingly distinct supermultiplets are related one to the other. One need only simultaneously exchange the purple and green colors of the links and then change the sign of the fermion Ψ_2 to see this. The supermultiplet corresponds to the string coordinates on the world sheet. On the other hand, if one starts with the adinkra in Fig 4(a), performs a simultaneous exchange of the green and purple colors of the links, followed by changing the sign of the fermion Ψ_2 , it does *not* become the adinkra in Fig. 4(d).

Finally, the adinkra in Fig. 4(d) corresponds to the projection of a 2D, $\mathcal{N} = (2,0)$ SUSY heterotic fermion supermultiplet that resides on the world sheet of a string [26,27].

So straight away the power of adinkras to unify distinct SUSY representations is made apparent.

We should also mention the two theories with only 2D, $\mathcal{N} = (2,0)$ SUSY cannot be made into theories that live on a 2D world sheet that possesses $\mathcal{N} = (1,1)$ SUSY. Many years ago, a result was derived that may be described as the “no two color ambidextrous bow-tie” theorem [16]. There it was shown that if one attempted to interpret the supermultiplets in Figs. 4(a) and 4(d) in the context of $\mathcal{N} = (1,1)$ SUSY on the world sheet. Lorentz invariance must be broken. This same result was more rigorously and mathematically extended in the works of [28,17].

In total, there are 16 distinct $\mathcal{GR}(2,2)$ valise adinkras as shown in Fig. 5. These are tabulated in terms of sign flips H_1^a and permutations S_2^μ where $a = 1, 2$ and $\mu = 1, 2$

$$H_1^a = \{(), (\bar{1})\} \quad , \quad S_2^\mu = \{(), (12)\} \quad . \quad (4.44)$$

Analogous to the BC_4 notation of [19] that was summarized in Sec. 2, all 16 adinkras in Fig. 5 are succinctly labeled as

$$L_I^{\pm a\mu b} = \pm H_1^a S_2^\mu L_I^{(0)} H_1^b \quad , \quad R_I^{\pm a\mu b} = (L_I^{\pm a\mu b})^T \quad , \quad (4.45)$$

where $L_I^{(0)}$ corresponds to the adinkra in Fig. 3 with adinkra matrices as in Eq. (4.38) and the T superscript means transpose. This is analogous to the BC_4 notation of [19] that was summarized in Sec. 2. Similar to the BC_4 case, there are isometries of $\mathcal{GR}(2,2)$ adinkras that reduce the total number of distinct adinkras from the 64 total possible BC_2 boson $\times BC_2$ fermion transformations to the 16 distinct adinkras in Fig. 5. These isometries are:

$$L_I = \mathcal{X} L_I \mathcal{Y} \quad (4.46a)$$

$$(\mathcal{X}, \mathcal{Y}) \in \begin{cases} ((\bar{1}), (\bar{1})) \\ ((\bar{1})(12), (\bar{1})(12)) \\ ((\bar{2})(12), (\bar{2})(12)) \\ ((\bar{1}2), (\bar{1}2)) \end{cases} \quad (4.46b)$$

These isometries are the reason that Eq. (4.45) can be written as it is, in terms of only flips on boson one, flops of bosons one and two, flips of fermion one, and an overall factor of plus or minus one. Altogether, these are the 16 possibilities that take a given starting $\mathcal{GR}(2,2)$ valise adinkra to all other possible $\mathcal{GR}(2,2)$ valise adinkras. There is nothing special about our choice for $L_I^{(0)} = L_I^{+111}$, it was chosen at random.

Next, we construct the 64 possible raisings of each of the 16 $\mathcal{GR}(2,2)$ adinkras as in Eq. (4.24):

$$L_I^{\pm a\mu b}(m, w) = M(m, w) L_I^{\pm a\mu b} \quad , \quad R_I^{\pm a\mu b}(\mu, w) = R_I^{\pm a\mu b} M(\mu^{-1}, w) \quad . \quad (4.47)$$

As in Eq. (4.43), we construct $B^{\pm a\mu b}$

$$B^{\pm a\mu b}(m, \mu, w) = \begin{pmatrix} L_2^{\pm a\mu b}(m, w) R_1^{\pm a\mu b}(\mu, w) & 0 \\ 0 & R_2^{\pm a\mu b}(\mu, w) L_1^{\pm a\mu b}(m, w) \end{pmatrix} \quad \text{no } a, \mu, b \text{ sum.} \quad (4.48)$$

This inspires us to calculate the eigenvalues of the following six matrices (no a, μ, b sum):

$$L_2^{\pm a\mu b}(m, w) R_1^{\pm a\mu b}(\mu, w) = -L_1^{\pm a\mu b}(m, w) R_2^{\pm a\mu b}(\mu, w) \quad , \quad (4.49)$$

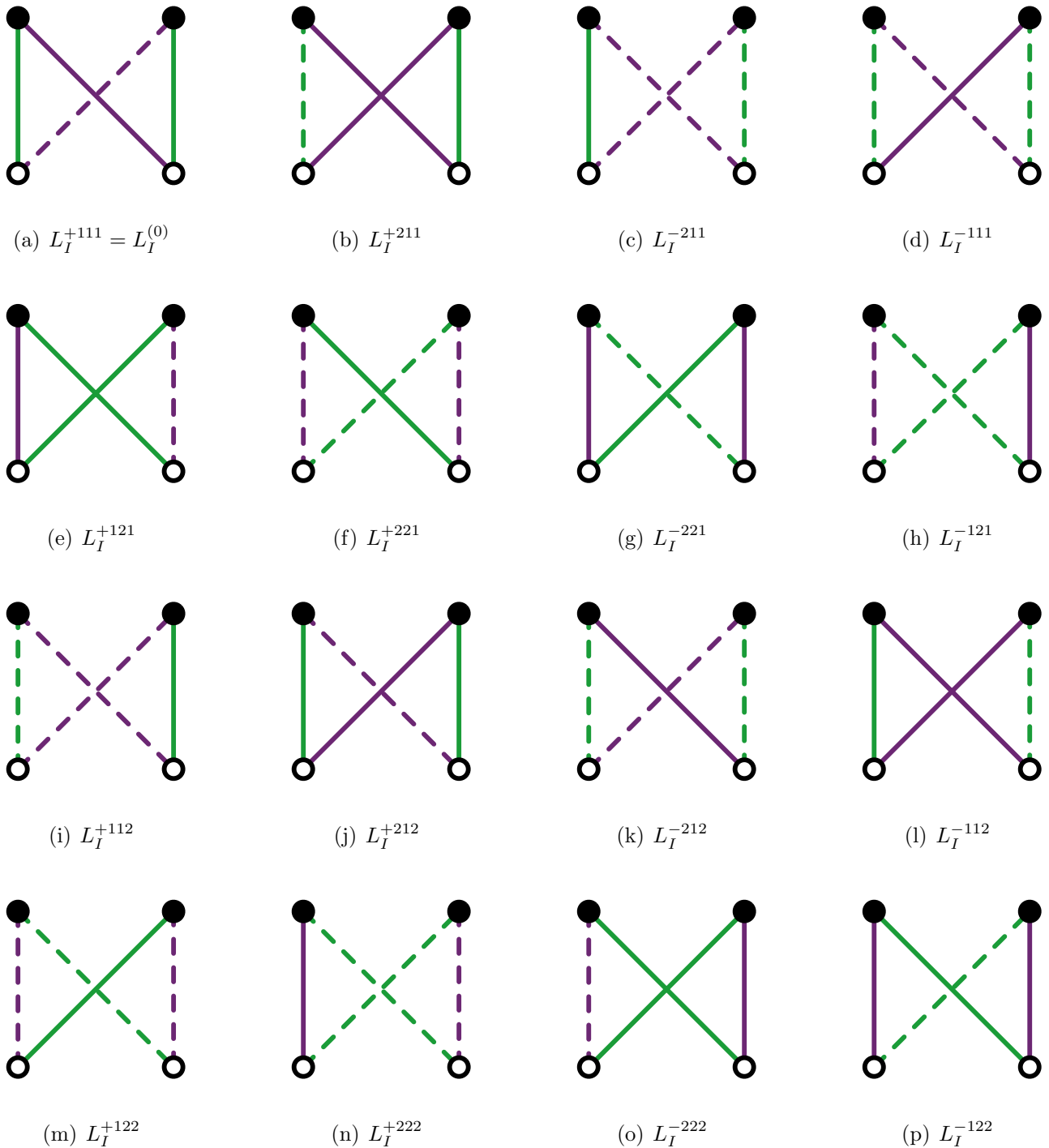


Figure 5: All 16 $\mathcal{GR}(2, 2)$ valise adinkras. The white nodes are bosons, the black fermions, in numerical left to right order as in Fig. 3.

$$M(m/\mu, w) = L_1^{\pm a\mu b}(m, w)R_1^{\pm a\mu b}(\mu, w) = L_2^{\pm a\mu b}(m, w)R_2^{\pm a\mu b}(\mu, w) \quad , \quad (4.50)$$

$$R_2^{\pm a\mu b}(\mu, w)L_1^{\pm a\mu b}(m, w) \quad , \quad R_1^{\pm a\mu b}(\mu, w)L_2^{\pm a\mu b}(m, w) \quad , \quad (4.51)$$

$$R_1^{\pm a\mu b}(\mu, w)L_1^{\pm a\mu b}(m, w) \quad , \quad R_2^{\pm a\mu b}(\mu, w)L_2^{\pm a\mu b}(m, w) \quad . \quad (4.52)$$

The calculation of these eigenvalues amounts to solving the following characteristic polynomials (no a, μ, b sum):

$$0 = \det \left(L_2^{\pm a\mu b}(m, w)R_1^{\pm a\mu b}(\mu, w) \pm \lambda I_{2 \times 2} \right) \quad , \quad (4.53)$$

$$0 = \det \left(M(m/\mu, w) - \lambda I_{2 \times 2} \right) \quad , \quad (4.54)$$

$$0 = \det \left(R_2^{\pm a\mu b}(\mu, w)L_1^{\pm a\mu b}(m, w) - \lambda I_{2 \times 2} \right) \quad , \quad (4.55)$$

$$0 = \det \left(R_1^{\pm a\mu b}(\mu, w)L_2^{\pm a\mu b}(m, w) - \lambda I_{2 \times 2} \right) \quad , \quad (4.56)$$

$$0 = \det \left(R_1^{\pm a\mu b}(\mu, w)L_1^{\pm a\mu b}(m, w) - \lambda I_{2 \times 2} \right) \quad , \quad (4.57)$$

$$0 = \det \left(R_2^{\pm a\mu b}(\mu, w)L_2^{\pm a\mu b}(m, w) - \lambda I_{2 \times 2} \right) \quad . \quad (4.58)$$

Owing to Eq. (4.49), the plus sign in Eq. (4.53) corresponds to the eigenvalues of $L_1^{\pm a\mu b}(m, w)R_2^{\pm a\mu b}(\mu, w)$.

4.2 Raised Boson Adinkras for $\mathcal{GR}(4, 4)$

Consider lifting one, two, three, and four bosonic nodes in a four-color valise adinkra with four bosons and four fermions. From Sec. 2, we have known there are 36,864 $\mathcal{GR}(4, 4)$ valise adinkras in total. Similar to the analysis in $\mathcal{GR}(2, 2)$ case, we define node raising operators:

$$M(m, 1) = \begin{pmatrix} m & 0 & 0 & 0 \\ 0 & 1 & 0 & 0 \\ 0 & 0 & 1 & 0 \\ 0 & 0 & 0 & 1 \end{pmatrix} \quad , \quad M(\mu^{-1}, 1) = \begin{pmatrix} \mu^{-1} & 0 & 0 & 0 \\ 0 & 1 & 0 & 0 \\ 0 & 0 & 1 & 0 \\ 0 & 0 & 0 & 1 \end{pmatrix} \quad , \quad (4.59)$$

$$M(m, 2) = \begin{pmatrix} 1 & 0 & 0 & 0 \\ 0 & m & 0 & 0 \\ 0 & 0 & 1 & 0 \\ 0 & 0 & 0 & 1 \end{pmatrix} \quad , \quad M(\mu^{-1}, 2) = \begin{pmatrix} 1 & 0 & 0 & 0 \\ 0 & \mu^{-1} & 0 & 0 \\ 0 & 0 & 1 & 0 \\ 0 & 0 & 0 & 1 \end{pmatrix} \quad , \quad (4.60)$$

$$M(m, 4) = \begin{pmatrix} 1 & 0 & 0 & 0 \\ 0 & 1 & 0 & 0 \\ 0 & 0 & m & 0 \\ 0 & 0 & 0 & 1 \end{pmatrix} \quad , \quad M(\mu^{-1}, 4) = \begin{pmatrix} 1 & 0 & 0 & 0 \\ 0 & 1 & 0 & 0 \\ 0 & 0 & \mu^{-1} & 0 \\ 0 & 0 & 0 & 1 \end{pmatrix} \quad , \quad (4.61)$$

$$M(m, 8) = \begin{pmatrix} 1 & 0 & 0 & 0 \\ 0 & 1 & 0 & 0 \\ 0 & 0 & 1 & 0 \\ 0 & 0 & 0 & m \end{pmatrix} \quad , \quad M(\mu^{-1}, 8) = \begin{pmatrix} 1 & 0 & 0 & 0 \\ 0 & 1 & 0 & 0 \\ 0 & 0 & 1 & 0 \\ 0 & 0 & 0 & \mu^{-1} \end{pmatrix} \quad , \quad (4.62)$$

For example, if we lift the i -th bosonic node, then the corresponding L_I and R_I for the lifted adinkra are

$$L_I(m, w) = M(m, w)L_I \quad , \quad R_I(\mu, w) = R_I M(\mu^{-1}, w) \quad , \quad (4.63)$$

where $w = 2^{i-1}$. Lifting more than one bosonic nodes can be described in the similar way. For example, the L_I and R_I matrices after lifting the $i - th$ and $j - th$ bosonic nodes are:

$$\begin{aligned} L_I(m, w) &= M(m, 2^{i-1})M(m, 2^{j-1})L_I \quad , \\ R_I(\mu, w) &= R_I M(\mu^{-1}, 2^{i-1})M(\mu^{-1}, 2^{j-1}) \quad . \end{aligned} \quad (4.64)$$

where node raising operators commute to each other, which means that lifting the $i - th$ node first then the $j - th$ node describes the same thing as lifting the $j - th$ node first then the $i - th$ node. In order to study isomorphic properties of non-valise adinkras, we study the B matrix

$$\begin{aligned} B &= \begin{pmatrix} 0 & L_4 \\ R_4 & 0 \end{pmatrix} \begin{pmatrix} 0 & L_3 \\ R_3 & 0 \end{pmatrix} \begin{pmatrix} 0 & L_2 \\ R_2 & 0 \end{pmatrix} \begin{pmatrix} 0 & L_1 \\ R_1 & 0 \end{pmatrix} \quad , \\ &= \begin{pmatrix} L_4 R_3 L_2 R_1 & 0 \\ 0 & R_4 L_3 R_2 L_1 \end{pmatrix} \quad . \end{aligned} \quad (4.65)$$

Next, we construct the 589,824 possible raisings of each of the 36,864 $\mathcal{GR}(4, 4)$ valise adinkras. Then we have

$$B_L(m, \mu, w) = L_4(m, w)R_3(\mu, w)L_2(m, w)R_1(\mu, w) \quad , \quad (4.66)$$

$$B_R(m, \mu, w) = R_4(\mu, w)L_3(m, w)R_2(\mu, w)L_1(m, w) \quad , \quad (4.67)$$

where the word parameter w can be 0, 1, 2, 3, \dots 15. The code (Listing 1) in the appendix B is the program to calculate the HYMNs, i.e. the eigenvalues of $B_L(m, \mu, w)$ and $B_R(m, \mu, w)$, for all 589,824 possible raisings. A summary using a *Mathematica* notebook can be found at the HEPThools [Data Repository](#) on GitHub.

5 Results

Let us define the mass ratio parameter ρ to connect m and μ ,

$$\rho \equiv \frac{m}{\mu} \quad . \quad (5.1)$$

We shall find that the eigenvalues of the matrices described previously will depend only on this ratio parameter.

5.1 HYMNs and Other Eigenvalues for $\mathcal{GR}(2, 2)$

As shown by Eq. (4.47), there are 64 possible $\mathcal{GR}(2, 2)$ valise and raised adinkras. The eigenvalues of $L_1(m, w)R_1(\mu, w)$, $L_2(m, w)R_1(\mu, w)$, $R_1(\mu, w)L_1(m, w)$, $R_1(\mu, w)L_2(m, w)$, $R_2(\mu, w)L_1(m, w)$, and $R_2(\mu, w)L_2(m, w)$ define eigenvalue equivalence classes of $\mathcal{GR}(2, 2)$ adinkras. We find

- all sixteen valise $\mathcal{GR}(2, 2)$ adinkras give the same eigenvalues:
 $L_1(m, w)R_1(\mu, w) : \{1, 1\}$; $L_2(m, w)R_1(\mu, w) : \{i, -i\}$; $R_1(\mu, w)L_1(m, w) : \{1, 1\}$;
 $R_1(\mu, w)L_2(m, w) : \{i, -i\}$; $R_2(\mu, w)L_1(m, w) : \{i, -i\}$; $R_2(\mu, w)L_2(m, w) : \{1, 1\}$
- all $\mathcal{GR}(2, 2)$ adinkras with one boson raised give the same eigenvalues:
 $L_1(m, w)R_1(\mu, w) : \{1, \rho\}$; $L_2(m, w)R_1(\mu, w) : \{i\sqrt{\rho}, -i\sqrt{\rho}\}$; $R_1(\mu, w)L_1(m, w) : \{1, \rho\}$;
 $R_1(\mu, w)L_2(m, w) : \{i\sqrt{\rho}, -i\sqrt{\rho}\}$; $R_2(\mu, w)L_1(m, w) : \{i\sqrt{\rho}, -i\sqrt{\rho}\}$; $R_2(\mu, w)L_2(m, w) : \{1, \rho\}$

- all $\mathcal{GR}(2, 2)$ adinkras with two bosons raised give the same eigenvalues:
 $L_1(m, w)R_1(\mu, w) : \{\rho, \rho\}$; $L_2(m, w)R_1(\mu, w) : \{i\rho, -i\rho\}$; $R_1(\mu, w)L_1(m, w) : \{\rho, \rho\}$;
 $R_1(\mu, w)L_2(m, w) : \{i\rho, -i\rho\}$; $R_2(\mu, w)L_1(m, w) : \{i\rho, -i\rho\}$; $R_2(\mu, w)L_2(m, w) : \{\rho, \rho\}$

These eigenvalue equivalence classes are summarized in Table 1.

Table 1: Eigenvalue Equivalence Classes of $\mathcal{GR}(2, 2)$

Type	w	Total Number	Eigenvalue Equivalence Class	# of Adinkras in Each Class
Valise Adinkras	0	16	all	16
One Boson Raised Adinkras	1,2	32	all	32
Two Bosons Raised Adinkras	3	16	all	16

5.2 HYMNs for $\mathcal{GR}(4, 4)$

For $\mathcal{GR}(4, 4)$, we focus specifically on HYMNs, i.e. the eigenvalues for $B_L(\rho, w)$ and $B_R(\rho, w)$, as no additional information was found for $\mathcal{GR}(2, 2)$ in for instance the eigenvalues of $L_2(m, w)R_1(m, w)$ that was not already present in the HYMNs. As $B_L(m, \mu, w)$ and $B_R(m, \mu, w)$ are found to depend only on ρ , we refer to these here as $B_L(\rho, w)$ and $B_R(\rho, w)$. We have calculated the HYMNs for all 589,824 possible valise and raised adinkras. We summarize the HYMN equivalence classes below.

1. 36,864 $\mathcal{GR}(4, 4)$ valise adinkras split into two classes: $\chi_o = \pm 1$, in each class adinkras give the same HYMNs
 $B_L(\rho, w) : \chi_o \{1, 1, 1, 1\}$; $B_R(\rho, w) : \chi_o \{-1, -1, -1, -1\}$
2. 147,456 $\mathcal{GR}(4, 4)$ adinkras with one boson raised split into two classes: $\chi_o = \pm 1$, in each class adinkras give the same HYMNs
 $B_L(\rho, w) : \chi_o \{1, 1, \rho, \rho\}$; $B_R(\rho, w) : \chi_o \{-1, -1, -\rho, -\rho\}$
3. 227,184 $\mathcal{GR}(4, 4)$ adinkras with two bosons raised split into six eigenvalue equivalence classes $EB_1^{(\chi_o)}$, $EB_2^{(\chi_o)}$, and $EB_3^{(\chi_o)}$. In each class, the matrices $B_L(\rho, w)$ and $B_R(\rho, w)$ have the same HYMNs
 $EB_1^{(\chi_o)} : B_L(\rho, w) : \chi_o \{\rho, \rho, \rho, \rho\}$; $B_R(\rho, w) : \chi_o \{-1, -1, -\rho^2, -\rho^2\}$
 $EB_2^{(\chi_o)} : B_L(\rho, w) : \chi_o \{1, 1, \rho^2, \rho^2\}$; $B_R(\rho, w) : \chi_o \{-\rho, -\rho, -\rho, -\rho\}$
 $EB_3^{(\chi_o)} : B_L(\rho, w) : \chi_o \{\rho, \rho, \rho, \rho\}$; $B_R(\rho, w) : \chi_o \{-\rho, -\rho, -\rho, -\rho\}$
4. 147,456 $\mathcal{GR}(4, 4)$ adinkras with three bosons raised split into two classes: $\chi_o = \pm 1$, in each class adinkras give the same HYMNs
 $B_L(\rho, w) : \chi_o \{\rho, \rho, \rho^2, \rho^2\}$; $B_R(\rho, w) : \chi_o \{-\rho, -\rho, -\rho^2, -\rho^2\}$
5. 36,864 $\mathcal{GR}(4, 4)$ adinkras with all four bosons raised split into two classes: $\chi_o = \pm 1$, in each class adinkras give the same HYMNs
 $B_L(\rho, w) : \chi_o \{\rho^2, \rho^2, \rho^2, \rho^2\}$; $B_R(\rho, w) : \chi_o \{-\rho^2, -\rho^2, -\rho^2, -\rho^2\}$

These eigenvalue equivalence classes are summarized in Table 2.

Table 2: HYMN Equivalence Classes of $\mathcal{GR}(4, 4)$

Type	w	Total Number	HYMN Equivalence Classes	# of Adinkras in Each Class
Valise Adinkras	0	36,864	$\chi_o = \pm 1$	18,432
One Boson Raised Adinkras	1,2,4,8	147,456	$\chi_o = \pm 1$	73,728
Two Bosons Raised Adinkras	3,5,6,9,10,12	221,184	$EB_1^{(\pm)}, EB_2^{(\pm)}, EB_3^{(\pm)}$	36,864
Three Bosons Raised Adinkras	7,11,13,14	147,456	$\chi_o = \pm 1$	73,728
Four Bosons Raised Adinkras	15	36,864	$\chi_o = \pm 1$	18,432

There is an interesting relationship between adinkras within the $EB_i^{(\pm)}$ equivalence classes for two raised bosons. For a given valise adinkra, raising bosons one and two are in the same equivalence class as raising bosons three and four. The same holds for raising one and three or two and four as well as for one and four or two and three. In terms of words, for a given valise adinkra raising two bosons with either the word code w or $15 - w$ will lead to the same equivalence class. Specifically, these word pairs are (3, 12), (5, 10) and (6, 9). It is important to note that this does not mean that all adinkras raised with word $w = 3$ have the same HYMNs as all adinkras raised with word $w = 12$, but merely that given a particular valise adinkra, raising with word $w = 3$ will lead to the same HYMNs as instead raising the same valise adinkra with word $w = 12$. Possibly, some adinkras raised with the word $w = 3$ may be in the same equivalence class as other adinkras raised with the word $w = 5$ for instance, it depends on how the valise adinkras are related by signed bosons and fermion permutations.

In order to relate this discussion back to the supermultiplets discussed in chapter three, let us make a series of observations about the structure of the superfields that describe them. When *no* node lowering is applied to the 4D, $\mathcal{N} = 1$ tensor supermultiplet or Hodge Dual # 3 chiral supermultiplet, under the action of projection to 1D, $N = 4$ supermultiplets, these are within the class of adinkras with $w = 0$. When *no* node lowering is applied to the 4D, $\mathcal{N} = 1$ vector supermultiplet, the Hodge Dual # 1, or Hodge Dual # 2 chiral 4D, $\mathcal{N} = 1$ chiral supermultiplets, under the action of projection to 1D, $N = 4$ supermultiplets, these are within the class of adinkras with $w = 1, 2, 4$, or 8. When *no* node lowering is applied to the 4D, $\mathcal{N} = 1$ chiral supermultiplet, under the action of projection to a 1D, $N = 4$ supermultiplet, it is within the class of adinkras with $w = 3, 5, 6, 9, 10$, and 12. When *no* node lowering is applied to the 4D, $\mathcal{N} = 1$ field strengths of the tensor supermultiplet, Hodge Dual # 1, or Hodge Dual # 2 chiral supermultiplet, under the action of projection to 1D, $N = 4$ supermultiplets, these are within the class of adinkras with $w = 7, 11, 13, 14$. The spinor field strengths for all of these supermultiplets correspond to $w = 15$.

6 Conclusion

In this paper, we introduced equivalence classes for non-valise adinkras that relate to isomorphisms of adinkras. We defined B -matrices and defined HYMNs as the eigenvalues of these matrices. Interestingly, the HYMNs seem to carry all information about isomorphisms in shape. To further the understanding of adinkra isomorphisms of non-valise adinkras, we have developed a program to calculate eigenvalues of B -matrices in the Python language that is given in appendix B. A summary of the findings of this program is given in a *Mathematica* notebook that can be found at the HEPThools [Data Repository](#) on GitHub.

From Figure 4, it was clear starting from the reference valise adinkra the number of other adinkras with lifted nodes that can be constructed from it occur as follows. There was one adinkra with no nodes lifted, two adinkras with one node lifted, and finally one adinkra with two nodes lifted. Looking vertically in the column that labels “Total Number” in Table 1, we see the ratios of 1:2:1, i. e. the binomial coefficient for two choose an integer. In turn this implies that the actions of lifting nodes versus using flips and flops to generate all sixty-four adinkras commute one with the other.

Looking vertically in the column that labels “Total Number” in Table 2, we see the ratios 1:4:6:4:1, i. e. the binomial coefficient for four choose an integer. As in the two color case this also implies that the actions of lifting nodes versus using flips and flops to generate all adinkras commute one with the other.

This analysis also provides a simple way to see the number⁵ of adinkras associated with BC_4 and with all possibility of raised nodes is equal to $4! \times 36,864 = 884,736$.

The observations in this work reveal that the HYMNs, i. e. the eigenvalues of the B -matrices for the adinkras investigated, can be used to cleanly partition these sets of adinkras into distinct classes. Apparently, the actions of the flipping and flopping operation preserve these classes. This offers an explicit route whereby considering instead of individual adinkras as the basis for higher dimensional supermultiplets, it is the emergent class structure of adinkras that provides such a basis.

The introduction of the matrix $M(m, w)$ as the nodal raising operator has implications for future directions of research. Previous mathematical “devices” introduced for the analysis of adinkras include holoraumy [30] and the Gadget [32]. But all such previous discussions have been restricted to valise adinkras. Clearly these can now be modified by appropriate introductions of $M(m, w)$ into their definitions. As well, future study of the holoraumy, Gadget, HYMNs, and χ_o all seems indicated to ascertain their dependence on adinkra dashing as well as the impacts of $M(m, w)$. Another class of questions to study is the generalization of this formalism to the cases where valise nodes can be lifted more than once. The simplest place to study this is for three-color adinkras. Finally with the introduction of $M(m, w)$ a re-examination of the work in [14] and [15] is also possible to be extended to the entire 36,864 BC_4 related adinkras.

⁵This number counts both $\chi_o = \pm 1$ sectors in the work of [24].

*“Don’t lower your expectations to meet your performance.
Raise your level of performance to meet your expectations.”*

- Ralph Marston

Added Note In Proof

After the completion of this work, the relevance of the research works in [38,39,40,41] were brought to our attention. The interested reader is referred to these papers to see the relation of “dressing matrices” (introduced in these works) and our height-raising factors.

Acknowledgments

This research is supported in part by the endowment of the Ford Foundation Professorship of Physics at Brown University. Yangrui Hu would like to acknowledge her participation in the second annual Brown University Adinkra Math/Phys Hangout” during 2017. This work was partially supported by the National Science Foundation grant PHY-1620074. S. J. G.’s research in the work was also supported in part by the endowment of the John S. Toll Professorship, the University of Maryland Center for String & Particle Theory, National Science Foundation Grant PHY-09-68854. S. J. G. acknowledges the generous support of the Roth Professorship and the very congenial and generous hospitality of the Dartmouth College physics department in the period of this investigation. Finally, we would like to acknowledge Mr. Isaac Friend for his cross-checking a previous version of the code used to sort the BC_4 related adinkras.

A Generating Minimal 1D SUSY Representations

When the results for $d_{\min}(N)$ (described in the introduction) are written more explicitly for values $1 \leq N \leq 16$, they can be expressed as shown in the first table.

Table 3: Number of Supercharges vs. Number of Bosons (or Fermions)

N	1	2	3	4	5	6	7	8	9	10	11	12	13	14	15	16
$d_{\min}(N)$	1	2	4	4	8	8	8	8	16	32	64	64	128	128	128	128

From this table we see there are some values of N such that as one goes from N to $N + 1$, the size of the L-matrices and R-matrices “jumps” by a factor of two. This occurs for all the N values in the sequence given by

$$1, 2, 4, 8, 9, 10, 12, 16, 17, 18, 20, 25, \dots \quad (\text{A.1})$$

and we can borrow language from nuclear physics⁶ and call these “magical” values of N .

This chart also illustrates the equation

$$d_{\min}(N + 8) = 16 d_{\min}(N) \quad , \quad (\text{A.2})$$

or more generally (going beyond the values of the table),

$$d_{\min}(N + 8m) = 16^m d_{\min}(N) \quad . \quad (\text{A.3})$$

This implies that the magical numbers are periodic with period 8. This is reminiscent of Bott periodicity, where the homotopy groups of the infinite dimensional real orthogonal group O is given by a periodic sequence of groups with periodicity $n \pmod{8}$: $\pi_k(O) = \pi_{k+8}(O)$ [36]. Here, the magic numbers are one more than the degrees in which these groups are non-trivial. The connection between these phenomena is due to the relationship of $\mathcal{GR}(d,N)$ algebras to Clifford algebras, with the latter also exhibiting the period 8 behavior [37].

In the following, we will describe the recursive algorithm introduced in [1,2] as well as bring our results in line with our current conventions and notation. This will also provide justifications for the formulae in (A.2) and (A.3).

As will be seen in each case when the value of N is “magical,” one L -matrix can be chosen to be equal to the corresponding R -matrix and both are symmetric under matrix transposition. In fact, this one matrix is taken to be the identity matrix. The remaining $(N - 1)$ L -matrices are equal to the negative of the corresponding R -matrices and both are antisymmetric under matrix transposition. The recursion construction only makes use of the antisymmetrical matrices that occur in the magical values of N .

⁶ See the webpage at [https://en.wikipedia.org/wiki/Magic_number_\(physics\)](https://en.wikipedia.org/wiki/Magic_number_(physics)) on-line.

For $N = 2$, there were given the set of 2×2 matrices:

$$\begin{aligned} L_1 &= \mathbf{I}_{2 \times 2} = R_1 \quad , \\ L_2 &= i\sigma^2 = -R_2 \quad . \end{aligned} \tag{A.4}$$

For $N = 4$, there were given two distinct minimal set of matrices that realize the $\mathcal{GR}(4, 4)$ algebra given by

$$\begin{aligned} L_1 &= \mathbf{I}_{2 \times 2} \otimes \mathbf{I}_{2 \times 2} = R_1 \quad , \\ L_2 &= i\sigma^1 \otimes \sigma^2 = -R_2 \quad , \\ L_3 &= i\sigma^2 \otimes \mathbf{I}_{2 \times 2} = -R_3 \quad , \\ L_4 &= -i\sigma^3 \otimes \sigma^2 = -R_4 \quad , \\ \\ \tilde{L}_1 &= \mathbf{I}_{2 \times 2} \otimes \mathbf{I}_{2 \times 2} = \tilde{R}_1 \quad , \\ \tilde{L}_2 &= i\sigma^2 \otimes \sigma^3 = -\tilde{R}_2 \quad , \\ \tilde{L}_3 &= -i\mathbf{I}_{2 \times 2} \otimes \sigma^2 = -\tilde{R}_3 \quad , \\ \tilde{L}_4 &= i\sigma^2 \otimes \sigma^1 = -\tilde{R}_4 \quad . \end{aligned} \tag{A.5}$$

Any three within each of these given sets can be used to cover the case of $N = 3$. For $N = 8$, a convenient set for our required matrices is given by,

$$\begin{aligned} L_1 &= \mathbf{I}_{2 \times 2} \otimes \mathbf{I}_{2 \times 2} \otimes \mathbf{I}_{2 \times 2} = R_1 \quad , \\ L_2 &= i\mathbf{I}_{2 \times 2} \otimes \sigma^3 \otimes \sigma^2 = -R_2 \quad , \\ L_3 &= i\sigma^3 \otimes \sigma^2 \otimes \mathbf{I}_{2 \times 2} = -R_3 \quad , \\ L_4 &= i\mathbf{I}_{2 \times 2} \otimes \sigma^1 \otimes \sigma^2 = -R_4 \quad , \\ L_5 &= i\sigma^1 \otimes \sigma^2 \otimes \mathbf{I}_{2 \times 2} = -R_5 \quad , \\ L_6 &= i\sigma^2 \otimes \mathbf{I}_{2 \times 2} \otimes \sigma^1 = -R_6 \quad , \\ L_7 &= i\sigma^2 \otimes \mathbf{I}_{2 \times 2} \otimes \sigma^3 = -R_7 \quad , \\ L_8 &= i\sigma^2 \otimes \sigma^2 \otimes \sigma^2 = -R_8 \quad . \end{aligned} \tag{A.6}$$

For the cases of $N = 5, 6$, and 7 , these can be formed by taking any subset consisting of $5, 6$, or 7 elements of the set of $N = 8$ matrices, respectively.

Finally, in the works of [1,2] the existence of a recursion formula⁷ generating matrix representations for arbitrary values of m and n in the formula $N = 8m + n$ (where m is any non-negative integer and n is an integer so that $1 \leq n \leq 8$) was given. We define,

$$\begin{aligned} L_1 &= \mathbf{I}_{2 \times 2} \otimes \mathbf{I}_{d_{\min}(n) \times d_{\min}(n)} \otimes \mathbf{I}_{d_{\min}(8m) \times d_{\min}(8m)} = R_1 \quad , \\ L_2 &= i\sigma^2 \otimes \mathbf{I}_{d_{\min}(n) \times d_{\min}(n)} \otimes \mathbf{I}_{d_{\min}(8m) \times d_{\min}(8m)} = -R_2 \quad , \\ L_{\hat{A}} &= \sigma^3 \otimes L_{\hat{A}}(n)_{d_{\min}(n) \times d_{\min}(n)} \otimes \mathbf{I}_{d_{\min}(8m) \times d_{\min}(8m)} = -R_{\hat{A}} \quad , \\ L_{\hat{M}} &= \sigma^1 \otimes \mathbf{I}_{d_{\min}(n) \times d_{\min}(n)} \otimes L_{\hat{M}}(8m)_{d_{\min}(8m) \times d_{\min}(8m)} = -R_{\hat{M}} \quad , \end{aligned} \tag{A.7}$$

and in the following we include discussion on why this works. However, we note there exist many ways to construct such recursion formulae. One source of this diversity in the fact that the roles of the σ^1 and σ^3 matrices can be “swapped.”

⁷The formulae which appear in (A.7) make corrections with regard to the modification $n \times n \rightarrow d_{\min}(n) \times d_{\min}(n)$.

Above, we have used the notation where $I_{d_{\min}(n) \times d_{\min}(n)}$ represents the $d_{\min}(n) \times d_{\min}(n)$ identity matrix for a given n where $d_{\min}(n)$ can be read from the function in (4.37) by putting $m = 0$. The matrices $L_{\widehat{A}}(n)_{d_{\min}(n) \times d_{\min}(n)}$ and $L_{\widehat{M}}(8m)_{d_{\min}(8m) \times d_{\min}(8m)}$ are only taken from the purely anti-symmetrical L-matrices for any value of N . Under this circumstance the index \widehat{A} is restricted and chosen to only run over those $L_{\widehat{A}}(n)$ matrices that are antisymmetric. The index \widehat{M} is restricted and chosen to only run over those $L_{\widehat{M}}(8m)_{d_{\min}(8m) \times d_{\min}(8m)}$ matrices that are antisymmetric matrices for the case of $N = 8m$. Application of this recursion formulae to the previous cases lead to the results reported in the following discussion. It is instructive to spend a bit of time on the topic of results that arise from the recursion formula in (A.7).

Clearly $9 = 8 + 1$ which implies for this case we should use the recursion formula with $m = 1$ and $n = 1$. For $n = 1$, $L_1 = R_1 = 1$. In particular this means that the second factor is absent. But also there are no $L_{\widehat{A}}(1)_{1 \times 1}$ matrices. In this case, the recursion formula (A.7) collapses to

$$\begin{aligned} L_1 &= I_{2 \times 2} \otimes I_{8 \times 8} = R_1 \quad , \\ L_{\widehat{A}} &= i\sigma^2 \otimes I_{8 \times 8} = -R_{\widehat{A}} \quad , \\ L_{\widehat{M}} &= \sigma^1 \otimes L_{\widehat{M}}(8) = -R_{\widehat{M}} \quad , \end{aligned} \tag{A.8}$$

and the $L_{\widehat{M}}(8)$ matrices are simply the last seven matrices as these are the anti-symmetrical ones in (A.6) for $N = 8$. Thus, for $N = 9$, we find the explicit form of the 16×16 matrices are given by:

$$\begin{aligned} L_1 &= I_{2 \times 2} \otimes I_{2 \times 2} \otimes I_{2 \times 2} \otimes I_{2 \times 2} = R_1 \quad , \\ L_2 &= i\sigma^2 \otimes I_{2 \times 2} \otimes I_{2 \times 2} \otimes I_{2 \times 2} = -R_2 \quad , \\ L_3 &= i\sigma^1 \otimes I_{2 \times 2} \otimes \sigma^3 \otimes \sigma^2 = -R_3 \quad , \\ L_4 &= i\sigma^1 \otimes \sigma^3 \otimes \sigma^2 \otimes I_{2 \times 2} = -R_4 \quad , \\ L_5 &= i\sigma^1 \otimes I_{2 \times 2} \otimes \sigma^1 \otimes \sigma^2 = -R_5 \quad , \\ L_6 &= i\sigma^1 \otimes \sigma^1 \otimes \sigma^2 \otimes I_{2 \times 2} = -R_6 \quad , \\ L_7 &= i\sigma^1 \otimes \sigma^2 \otimes I_{2 \times 2} \otimes \sigma^1 = -R_7 \quad , \\ L_8 &= i\sigma^1 \otimes \sigma^2 \otimes I_{2 \times 2} \otimes \sigma^3 = -R_8 \quad , \\ L_9 &= i\sigma^1 \otimes \sigma^2 \otimes \sigma^2 \otimes \sigma^2 = -R_9 \quad . \end{aligned} \tag{A.9}$$

Since $10 = 8 + 2$, this implies for this case we have $m = 1$ and $n = 2$. The L-matrices and R-matrices for $n = 2$ appear in (A.4). Thus, we have $I_{d_{\min}(n) \times d_{\min}(n)} = I_{2 \times 2}$ and the set $L_{\widehat{A}}(2 \times 2)$ consists of the single element $i\sigma^2$. Using these, the recursion formula yields

$$\begin{aligned} L_1 &= I_{2 \times 2} \otimes I_{2 \times 2} \otimes I_{8 \times 8} = R_1 \quad ; \\ L_2 &= i\sigma^2 \otimes I_{2 \times 2} \otimes I_{8 \times 8} = -R_2 \quad ; \\ L_3 &= i\sigma^3 \otimes \sigma^2 \otimes I_{8 \times 8} = -R_3 \quad ; \\ L_{\widehat{M}} &= \sigma^1 \otimes I_{2 \times 2} \otimes L_{\widehat{M}}(8) = -R_{\widehat{M}} \quad ; \end{aligned} \tag{A.10}$$

where $L_{\widehat{M}}(8)$ once again consists of the seven antisymmetrical matrices that occur in the case of 8×8 matrices that are explicitly exhibited in (A.6).

As will be described in the equation (A.7), the recursion formula generates successively larger and larger matrices that satisfy a set of algebraic conditions. These conditions are those required to realize N supercharges linearly on d_{\min} bosons and the same number of fermions. It also plays

the very important role of extending the matrix representation that have $N \leq 8$ to those which have $N > 8$. The recursion formula is also the basis for the answer to the first question raised in this work as well as the origin of the “magic number” sequence.

More explicitly for $N = 10$ we able to find a 32×32 representation:

$$\begin{aligned}
L_1 &= \mathbf{I}_{2 \times 2} \otimes \mathbf{I}_{2 \times 2} \otimes \mathbf{I}_{2 \times 2} \otimes \mathbf{I}_{2 \times 2} \otimes \mathbf{I}_{2 \times 2} = R_1 , \\
L_2 &= i\sigma^2 \otimes \mathbf{I}_{2 \times 2} \otimes \mathbf{I}_{2 \times 2} \otimes \mathbf{I}_{2 \times 2} \otimes \mathbf{I}_{2 \times 2} = -R_2 , \\
L_3 &= i\sigma^3 \otimes \sigma^2 \otimes \mathbf{I}_{2 \times 2} \otimes \mathbf{I}_{2 \times 2} \otimes \mathbf{I}_{2 \times 2} = -R_3 , \\
L_4 &= i\sigma^1 \otimes \mathbf{I}_{2 \times 2} \otimes \mathbf{I}_{2 \times 2} \otimes \sigma^3 \otimes \sigma^2 = -R_4 , \\
L_5 &= i\sigma^1 \otimes \mathbf{I}_{2 \times 2} \otimes \sigma^3 \otimes \sigma^2 \otimes \mathbf{I}_{2 \times 2} = -R_5 , \\
L_6 &= i\sigma^1 \otimes \mathbf{I}_{2 \times 2} \otimes \mathbf{I}_{2 \times 2} \otimes \sigma^1 \otimes \sigma^2 = -R_6 , \\
L_7 &= i\sigma^1 \otimes \mathbf{I}_{2 \times 2} \otimes \sigma^1 \otimes \sigma^2 \otimes \mathbf{I}_{2 \times 2} = -R_7 , \\
L_8 &= i\sigma^1 \otimes \mathbf{I}_{2 \times 2} \otimes \sigma^2 \otimes \mathbf{I}_{2 \times 2} \otimes \sigma^1 = -R_8 , \\
L_9 &= i\sigma^1 \otimes \mathbf{I}_{2 \times 2} \otimes \sigma^2 \otimes \mathbf{I}_{2 \times 2} \otimes \sigma^3 = -R_9 , \\
L_{10} &= i\sigma^1 \otimes \mathbf{I}_{2 \times 2} \otimes \sigma^2 \otimes \sigma^2 \otimes \sigma^2 = -R_{10} .
\end{aligned} \tag{A.11}$$

The next magical value is the $N = 12$ case to lead to a 64×64 representation and $12 = 8 + 4$, implies for this case we have $m = 1$ and $n = 4$. Thus, we have $\mathbf{I}_{d_{\min}(n) \times d_{\min}(n)} = \mathbf{I}_{4 \times 4}$, the $L_{\widehat{A}}(4 \times 4)$ set consists of the final three elements from the matrices that appear in (A.5), and the set $L_{\widehat{M}}(8 \times 8)$ set consists of the final seven elements from the matrices that appear in (A.6).

$$\begin{aligned}
L_1 &= \mathbf{I}_{2 \times 2} \otimes \mathbf{I}_{4 \times 4} \otimes \mathbf{I}_{8 \times 8} = R_1 , \\
L_2 &= i\sigma^2 \otimes \mathbf{I}_{4 \times 4} \otimes \mathbf{I}_{8 \times 8} = -R_2 , \\
L_p &= \sigma^3 \otimes L_p(4) \otimes \mathbf{I}_{8 \times 8} = -R_p , \\
L_q &= \sigma^1 \otimes \mathbf{I}_{4 \times 4} \otimes L_q(8) = -R_q ,
\end{aligned} \tag{A.12}$$

where we have used the compact notation to efficiently express the forms of the appropriate 64×64 matrices. In this expression, the index p takes on the values of $p = 3, 4$, and 5 while the index $q = 6, \dots, 12$. More explicitly this becomes

$$\begin{aligned}
L_1 &= \mathbf{I}_{2 \times 2} \otimes \mathbf{I}_{2 \times 2} \otimes \mathbf{I}_{2 \times 2} \otimes \mathbf{I}_{2 \times 2} \otimes \mathbf{I}_{2 \times 2} \otimes \mathbf{I}_{2 \times 2} = R_1 , \\
L_2 &= i\sigma^2 \otimes \mathbf{I}_{2 \times 2} \otimes \mathbf{I}_{2 \times 2} \otimes \mathbf{I}_{2 \times 2} \otimes \mathbf{I}_{2 \times 2} \otimes \mathbf{I}_{2 \times 2} = -R_2 , \\
L_3 &= i\sigma^3 \otimes \sigma^1 \otimes \sigma^2 \otimes \mathbf{I}_{2 \times 2} \otimes \mathbf{I}_{2 \times 2} \otimes \mathbf{I}_{2 \times 2} = -R_3 , \\
L_4 &= i\sigma^3 \otimes \sigma^2 \otimes \mathbf{I}_{2 \times 2} \otimes \mathbf{I}_{2 \times 2} \otimes \mathbf{I}_{2 \times 2} \otimes \mathbf{I}_{2 \times 2} = -R_4 , \\
L_5 &= i\sigma^3 \otimes \sigma^3 \otimes \sigma^2 \otimes \mathbf{I}_{2 \times 2} \otimes \mathbf{I}_{2 \times 2} \otimes \mathbf{I}_{2 \times 2} = -R_5 , \\
L_6 &= i\sigma^1 \otimes \mathbf{I}_{2 \times 2} \otimes \mathbf{I}_{2 \times 2} \otimes \mathbf{I}_{2 \times 2} \otimes \sigma^3 \otimes \sigma^2 = -R_6 , \\
L_7 &= i\sigma^1 \otimes \mathbf{I}_{2 \times 2} \otimes \mathbf{I}_{2 \times 2} \otimes \sigma^3 \otimes \sigma^2 \otimes \mathbf{I}_{2 \times 2} = -R_7 , \\
L_8 &= i\sigma^1 \otimes \mathbf{I}_{2 \times 2} \otimes \mathbf{I}_{2 \times 2} \otimes \mathbf{I}_{2 \times 2} \otimes \sigma^1 \otimes \sigma^2 = -R_8 , \\
L_9 &= i\sigma^1 \otimes \mathbf{I}_{2 \times 2} \otimes \mathbf{I}_{2 \times 2} \otimes \sigma^2 \otimes \sigma^3 \otimes \mathbf{I}_{2 \times 2} = -R_9 , \\
L_{10} &= i\sigma^1 \otimes \mathbf{I}_{2 \times 2} \otimes \mathbf{I}_{2 \times 2} \otimes \sigma^2 \otimes \mathbf{I}_{2 \times 2} \otimes \sigma^1 = -R_{10} , \\
L_{11} &= i\sigma^1 \otimes \mathbf{I}_{2 \times 2} \otimes \mathbf{I}_{2 \times 2} \otimes \sigma^2 \otimes \mathbf{I}_{2 \times 2} \otimes \sigma^3 = -R_{11} , \\
L_{12} &= i\sigma^1 \otimes \mathbf{I}_{2 \times 2} \otimes \mathbf{I}_{2 \times 2} \otimes \sigma^2 \otimes \sigma^2 \otimes \sigma^2 = -R_{12} .
\end{aligned} \tag{A.13}$$

The case of $N = 11$ is contained as a subset.

The final explicit result that we present is for $N = 16$, where we have a 128×128 representation of the $N = 16$ supersymmetry algebra:

$$\begin{aligned}
L_1 &= \mathbb{I}_{2 \times 2} \otimes \mathbb{I}_{8 \times 8} \otimes \mathbb{I}_{8 \times 8} = R_1 \quad , \\
L_2 &= i\sigma^2 \otimes \mathbb{I}_{8 \times 8} \otimes \mathbb{I}_{8 \times 8} = -R_2 \quad , \\
L_r &= \sigma^3 \otimes L_r(8) \otimes \mathbb{I}_{8 \times 8} = -R_r \quad , \\
L_s &= \sigma^1 \otimes \mathbb{I}_{8 \times 8} \otimes L_s(8) = -R_s \quad ,
\end{aligned} \tag{A.14}$$

where we have again used a compact notation to efficiently express the forms of the appropriate 128×128 matrices. In this expression, the index r takes on the values of $r = 3, \dots, 9$ while the index $s = 10, \dots, 16$. Expanding this out completely yields,

$$\begin{aligned}
L_1 &= \mathbb{I}_{2 \times 2} \otimes \mathbb{I}_{2 \times 2} \otimes \mathbb{I}_{2 \times 2} \otimes \mathbb{I}_{2 \times 2} \otimes \mathbb{I}_{2 \times 2} \otimes \mathbb{I}_{2 \times 2} \otimes \mathbb{I}_{2 \times 2} \otimes \mathbb{I}_{2 \times 2} = R_1 \quad , \\
L_2 &= i\sigma^2 \otimes \mathbb{I}_{2 \times 2} \otimes \mathbb{I}_{2 \times 2} \otimes \mathbb{I}_{2 \times 2} \otimes \mathbb{I}_{2 \times 2} \otimes \mathbb{I}_{2 \times 2} \otimes \mathbb{I}_{2 \times 2} \otimes \mathbb{I}_{2 \times 2} = -R_2 \quad , \\
L_3 &= i\sigma^3 \otimes \mathbb{I}_{2 \times 2} \otimes \sigma^3 \otimes \sigma^2 \otimes \mathbb{I}_{2 \times 2} \otimes \mathbb{I}_{2 \times 2} \otimes \mathbb{I}_{2 \times 2} \otimes \mathbb{I}_{2 \times 2} = -R_3 \quad , \\
L_4 &= i\sigma^3 \otimes \sigma^3 \otimes \sigma^2 \otimes \mathbb{I}_{2 \times 2} \otimes \mathbb{I}_{2 \times 2} \otimes \mathbb{I}_{2 \times 2} \otimes \mathbb{I}_{2 \times 2} = -R_4 \quad , \\
L_5 &= i\sigma^3 \otimes \mathbb{I}_{2 \times 2} \otimes \sigma^1 \otimes \sigma^2 \otimes \mathbb{I}_{2 \times 2} \otimes \mathbb{I}_{2 \times 2} \otimes \mathbb{I}_{2 \times 2} \otimes \mathbb{I}_{2 \times 2} = -R_5 \quad , \\
L_6 &= i\sigma^3 \otimes \sigma^1 \otimes \sigma^2 \otimes \mathbb{I}_{2 \times 2} \otimes \mathbb{I}_{2 \times 2} \otimes \mathbb{I}_{2 \times 2} \otimes \mathbb{I}_{2 \times 2} = -R_6 \quad , \\
L_7 &= i\sigma^3 \otimes \sigma^2 \otimes \mathbb{I}_{2 \times 2} \otimes \sigma^1 \otimes \mathbb{I}_{2 \times 2} \otimes \mathbb{I}_{2 \times 2} \otimes \mathbb{I}_{2 \times 2} = -R_7 \quad , \\
L_8 &= i\sigma^3 \otimes \sigma^2 \otimes \mathbb{I}_{2 \times 2} \otimes \sigma^3 \otimes \mathbb{I}_{2 \times 2} \otimes \mathbb{I}_{2 \times 2} \otimes \mathbb{I}_{2 \times 2} = -R_8 \quad , \\
L_9 &= i\sigma^3 \otimes \sigma^2 \otimes \sigma^2 \otimes \sigma^2 \otimes \mathbb{I}_{2 \times 2} \otimes \mathbb{I}_{2 \times 2} \otimes \mathbb{I}_{2 \times 2} = -R_9 \quad , \\
L_{10} &= i\sigma^1 \otimes \mathbb{I}_{2 \times 2} \otimes \mathbb{I}_{2 \times 2} \otimes \mathbb{I}_{2 \times 2} \otimes \mathbb{I}_{2 \times 2} \otimes \mathbb{I}_{2 \times 2} \otimes \sigma^3 \otimes \sigma^2 = -R_{10} \quad , \\
L_{11} &= i\sigma^1 \otimes \mathbb{I}_{2 \times 2} \otimes \mathbb{I}_{2 \times 2} \otimes \mathbb{I}_{2 \times 2} \otimes \sigma^3 \otimes \sigma^2 \otimes \mathbb{I}_{2 \times 2} = -R_{11} \quad , \\
L_{12} &= i\sigma^1 \otimes \mathbb{I}_{2 \times 2} \otimes \mathbb{I}_{2 \times 2} \otimes \mathbb{I}_{2 \times 2} \otimes \mathbb{I}_{2 \times 2} \otimes \sigma^1 \otimes \sigma^2 = -R_{12} \quad , \\
L_{13} &= i\sigma^1 \otimes \mathbb{I}_{2 \times 2} \otimes \mathbb{I}_{2 \times 2} \otimes \mathbb{I}_{2 \times 2} \otimes \sigma^1 \otimes \sigma^2 \otimes \mathbb{I}_{2 \times 2} = -R_{13} \quad , \\
L_{14} &= i\sigma^1 \otimes \mathbb{I}_{2 \times 2} \otimes \mathbb{I}_{2 \times 2} \otimes \mathbb{I}_{2 \times 2} \otimes \sigma^2 \otimes \mathbb{I}_{2 \times 2} \otimes \sigma^1 = -R_{14} \quad , \\
L_{15} &= i\sigma^1 \otimes \mathbb{I}_{2 \times 2} \otimes \mathbb{I}_{2 \times 2} \otimes \mathbb{I}_{2 \times 2} \otimes \sigma^2 \otimes \mathbb{I}_{2 \times 2} \otimes \sigma^3 = -R_{15} \quad , \\
L_{16} &= i\sigma^1 \otimes \mathbb{I}_{2 \times 2} \otimes \mathbb{I}_{2 \times 2} \otimes \mathbb{I}_{2 \times 2} \otimes \sigma^2 \otimes \sigma^2 \otimes \sigma^2 = -R_{16} \quad .
\end{aligned} \tag{A.15}$$

The cases of $N = 13, 14$, and 15 are contained as subsets.

A careful comparison between all the results above and those presented in the works of [1,2] shows they are not identical. While both sets of results are correct, what we have done in the present work is to *actually* use the recursion formula to generate the cases of $9 \leq N \leq 16$.

B Original script for the program in the Python language

Listing 1: Original script for the program in the Python language

```
from sympy import *
import sympy as sp
import numpy as np
#define output file
5 file = open('GR(4,4)-Feb27_36864_output.txt', 'w')

# calculate eigenvalues of B matrices for one adinkra
def calculation_Bmatrix_eigenvalue(L1, L2, L3, L4):

10     # Get R matrix

    R1 = np.transpose(L1)
    R2 = np.transpose(L2)
    R3 = np.transpose(L3)
15    R4 = np.transpose(L4)

    # define m_i, nu_i = mu_i^{-1}

    m1 = sp.Symbol('m')
20    m2 = sp.Symbol('m')
    m3 = sp.Symbol('m')
    m4 = sp.Symbol('m')
    nu1 = sp.Symbol('nu')
    nu2 = sp.Symbol('nu')
25    nu3 = sp.Symbol('nu')
    nu4 = sp.Symbol('nu')

    # define lifting matrice
    P_L_1 = np.diag((m1,1,1,1))
30    P_L_2 = np.diag((1,m2,1,1))
    P_L_3 = np.diag((1,1,m3,1))
    P_L_4 = np.diag((1,1,1,m4))
    P_R_1 = np.diag((nu1,1,1,1))
    P_R_2 = np.diag((1,nu2,1,1))
35    P_R_3 = np.diag((1,1,nu3,1))
    P_R_4 = np.diag((1,1,1,nu4))

    #calculate B1, B2 matrix for 1+4+6+4+1 cases
40    and output their eigenvalues
    #B1 = L4*R3*L2*R1
    #B2 = R4*L3*R2*L1
```

```

# lift zero boson
45 B1_lift0 = np.mat(L4)*np.mat(R3)*np.mat(L2)*np.mat(R1)
    B2_lift0 = np.mat(R4)*np.mat(L3)*np.mat(R2)*np.mat(L1)

file.write('lift zero boson: \n')
B1_lift0_eigen1, B1_lift0_eigen2, B1_lift0_eigen3,
50 B1_lift0_eigen4, diag1 = calculate_eigenvalues(B1_lift0)
    B2_lift0_eigen1, B2_lift0_eigen2, B2_lift0_eigen3,
    B2_lift0_eigen4, diag2 = calculate_eigenvalues(B2_lift0)
file.write('eigenvalues for B1:' + ' ' +
55         + str(B1_lift0_eigen1) + ' ' + str(B1_lift0_eigen2)
         + ' ' + str(B1_lift0_eigen3) + ' '
         + str(B1_lift0_eigen4) + "\n")
file.write('eigenvalues for B2:' + ' ' +
60         + str(B2_lift0_eigen1) + ' ' + str(B2_lift0_eigen2)
         + ' ' + str(B2_lift0_eigen3) + ' '
         + str(B2_lift0_eigen4) + "\n")

#lift i-th boson (i = 1,2,3,4)
for i in (1,2,3,4):

65     locals()['B1_lift' + str(i)] = np.mat(locals()
        ['P_L_' + str(i)])*np.mat(L4)*np.mat(R3)*
        np.mat(locals()['P_R_' + str(i)])*np.mat(locals()
        ['P_L_' + str(i)])*np.mat(L2)*np.mat(R1)
        *np.mat(locals()['P_R_' + str(i)])
70     locals()['B2_lift' + str(i)] = np.mat(R4)
        *np.mat(locals()['P_R_' + str(i)])
        *np.mat(locals()['P_L_' + str(i)])
        *np.mat(L3)*np.mat(R2)*np.mat(locals()
        ['P_R_' + str(i)])*np.mat(locals()
75     ['P_L_' + str(i)])*np.mat(L1)

file.write('lift %d-th boson: \n'%i)
locals()['B1_lift' + str(i) + '_eigen1'],
locals()['B1_lift' + str(i) + '_eigen2'],
80 locals()['B1_lift' + str(i) + '_eigen3'],
    locals()['B1_lift' + str(i) + '_eigen4'],
    d= calculate_eigenvalues(locals()['B1_lift' + str(i)])
    locals()['B2_lift' + str(i) + '_eigen1'],
    locals()['B2_lift' + str(i) + '_eigen2'],
85 locals()['B2_lift' + str(i) + '_eigen3'],
    locals()['B2_lift' + str(i) + '_eigen4'],
    d= calculate_eigenvalues(locals()['B2_lift' + str(i)])
file.write('eigenvalues for B1:' + ' ' +
90         + str(locals()['B1_lift' + str(i)

```

```

90         + '_eigen1'])+ ' ' + str(locals()
        ['B1_lift' + str(i) + '_eigen2'])
        + ' ' + str(locals()['B1_lift'
        + str(i) + '_eigen3'])+ ' '
        + str(locals()['B1_lift' + str(i)
95         + '_eigen4']) + "\n")
file.write('eigenvalues for B2:' + ' '
        + str(locals()['B2_lift' + str(i)
        + '_eigen1'])+ ' ' + str(locals()
        ['B2_lift' + str(i) + '_eigen2'])
100     + ' ' + str(locals()['B2_lift'
        + str(i) + '_eigen3'])+ ' '
        + str(locals()['B2_lift' + str(i)
        + '_eigen4']) + "\n")

105
#lift (1,2) (1,3) (1,4) (2,3) (2,4) (3,4) bosons
for i in (1,2,3):
    for j in (2,3,4):
110         if i<j :

        locals()['B1_lift' + str(i)+ str(j)] =
        np.mat(locals()['P_L_' + str(i)])
        *np.mat(locals()['P_L_' + str(j)])
        *np.mat(L4)*np.mat(R3)*np.mat(locals()
115         ['P_R_' + str(i)])*np.mat(locals()
        ['P_R_' + str(j)])*np.mat(locals()
        ['P_L_' + str(i)])*np.mat(locals()
        ['P_L_' + str(j)])*np.mat(L2)*np.mat(R1)
        *np.mat(locals()['P_R_' + str(i)])
120         *np.mat(locals()['P_R_' + str(j)])
        locals()['B2_lift' + str(i)+ str(j)] =
        np.mat(R4)*np.mat(locals()['P_R_'
        + str(i)])*np.mat(locals()['P_R_'
        + str(j)])*np.mat(locals()['P_L_'
125         + str(i)])*np.mat(locals()['P_L_'
        + str(j)])*np.mat(L3)*np.mat(R2)
        *np.mat(locals()['P_R_' + str(i)])
        *np.mat(locals()['P_R_' + str(j)])
        *np.mat(locals()['P_L_' + str(i)])
130         *np.mat(locals()['P_L_' + str(j)])
        *np.mat(L1)

        file.write('lift (%d, %d)-th bosons: \n'%(i,j))
135         locals()['B1_lift' + str(i) + str(j) + '_eigen1'],

```

140

```

locals()['B1_lift' + str(i)+ str(j) + '_eigen2'],
locals()['B1_lift' + str(i)+ str(j) + '_eigen3'],
locals()['B1_lift' + str(i)+ str(j) + '_eigen4'],
d= calculate_eigenvalues(locals()['B1_lift'
+ str(i)+ str(j)])

```

145

```

locals()['B2_lift' + str(i) + str(j) + '_eigen1'],
locals()['B2_lift' + str(i)+ str(j) + '_eigen2'],
locals()['B2_lift' + str(i)+ str(j) + '_eigen3'],
locals()['B2_lift' + str(i)+ str(j) + '_eigen4'],
d= calculate_eigenvalues(locals()['B2_lift'
+ str(i)+ str(j)])

```

150

```

file.write('eigenvalues for B1:'+ ' '
+ str(locals()['B1_lift' + str(i)
+ str(j) + '_eigen1']))+ ' '
+ str(locals()['B1_lift' + str(i)
+ str(j) + '_eigen2']))+ ' '
+ str(locals()['B1_lift' + str(i)
+ str(j) + '_eigen3']))+ ' '
+ str(locals()['B1_lift' + str(i)
+ str(j) + '_eigen4'])) + "\n"

```

155

```

file.write('eigenvalues for B2:'+ ' '
+ str(locals()['B2_lift' + str(i)
+ str(j) + '_eigen1']))+ ' '
+ str(locals()['B2_lift' + str(i)
+ str(j) + '_eigen2']))+ ' '
+ str(locals()['B2_lift' + str(i)
+ str(j) + '_eigen3']))+ ' '
+ str(locals()['B2_lift' + str(i)
+ str(j) + '_eigen4'])) + "\n"

```

160

165

```

#lift (1,2,3) (1,2,4) (1,3,4) (2,3,4) bosons, (color = 1,2,3,4)

```

```

for i in (1,2):

```

170

```

    for j in (2,3):

```

```

        for k in (3,4):

```

```

            if i<j<k :

```

175

```

                locals()['B1_lift' + str(i)+ str(j)
+ str(k)] = np.mat(locals()['P_L_'
+ str(i)])*np.mat(locals()['P_L_'
+ str(j)])*np.mat(locals()['P_L_'
+ str(k)])*np.mat(L4)*np.mat(R3)
                *np.mat(locals()['P_R_' + str(i)])
                *np.mat(locals()['P_R_' + str(j)])
                *np.mat(locals()['P_R_' + str(k)])
                *np.mat(locals()['P_L_' + str(i)])
                *np.mat(locals()['P_L_' + str(j)])

```

180

185

190

195

200

205

210

215

220

225

```

        *np.mat(locals()['P_L_' + str(k)])
        *np.mat(L2)*np.mat(R1)*np.mat
        (locals()['P_R_' + str(i)])
        *np.mat(locals()['P_R_' + str(j)])
        *np.mat(locals()['P_R_' + str(k)])
locals()['B2_lift' + str(i)+ str(j)
+ str(k)] = np.mat(R4)*np.mat(locals()
        ['P_R_' + str(i)]*np.mat(locals()
        ['P_R_' + str(j)]*np.mat(locals()
        ['P_R_' + str(k)]*np.mat(locals()
        ['P_L_' + str(i)]*np.mat(locals()
        ['P_L_' + str(j)]*np.mat(locals()
        ['P_L_' + str(k)]*np.mat(L3)
        *np.mat(R2)*np.mat(locals()['P_R_'
        + str(i)]*np.mat(locals()['P_R_'
        + str(j)]*np.mat(locals()['P_R_'
        + str(k)]*np.mat(locals()['P_L_'
        + str(i)]*np.mat(locals()['P_L_'
        + str(j)]*np.mat(locals()['P_L_'
        + str(k)]*np.mat(L1)

file.write('lift (%d, %d, %d)-th
        bosons: \n'%(i,j,k))
locals()['B1_lift' + str(i) + str(j)
+ str(k) + '_eigen1'], locals()
['B1_lift' + str(i)+ str(j)+ str(k)
+ '_eigen2'], locals()['B1_lift'
+ str(i)+ str(j)+ str(k) + '_eigen3'],
        locals()['B1_lift' + str(i)+ str(j)
        + str(k) + '_eigen4'],
        d= calculate_eigenvalues(locals()
        ['B1_lift' + str(i)+ str(j)+ str(k)])
locals()['B2_lift' + str(i) + str(j)
+ str(k) + '_eigen1'], locals()
['B2_lift' + str(i)+ str(j)+ str(k)
+ '_eigen2'], locals()['B2_lift'
+ str(i)+ str(j)+ str(k) + '_eigen3'],
        locals()['B2_lift' + str(i)+ str(j)
        + str(k) + '_eigen4'], d
        = calculate_eigenvalues(locals()
        ['B2_lift' + str(i)+ str(j)+ str(k)])
file.write('eigenvalues for B1:'
        + ' ' + str(locals()['B1_lift'
        + str(i)+ str(j)+ str(k)
        + '_eigen1'])+ ' ' +
        str(locals()['B1_lift' +

```



```

                str(i)+ str(j)+ str(k)
                + '_eigen2'])+ ' ' +
230 str(locals()['B1_lift' + str(i)
                + str(j)+ str(k) + '_eigen3'])
                + ' ' + str(locals()['B1_lift'
                + str(i)+ str(j)+ str(k)
                + '_eigen4']) + "\n")
235 file.write('eigenvalues for B2:'
                + ' ' + str(locals()['B2_lift'
                + str(i)+ str(j)+ str(k) +
                '_eigen1'])+ ' ' +
                str(locals()['B2_lift' + str(i)
240 + str(j)+ str(k) + '_eigen2'])
                + ' ' + str(locals()['B2_lift'
                + str(i)+ str(j)+ str(k)
                + '_eigen3'])+ ' ' +
                str(locals()['B2_lift' + str(i)
245 + str(j)+ str(k) + '_eigen4'])
                + "\n")

#lift (1,2,3,4) bosons, (color = 1,2,3,4)
250 B1_lift1234 = np.mat(locals()['P_L_' + str(1)])
                *np.mat(locals()['P_L_' + str(2)])*np.mat(locals
                (')['P_L_' + str(3)])*np.mat(locals()['P_L_'
                + str(4)])*np.mat(L4)*np.mat(R3)*np.mat
                (locals()['P_R_' + str(1)])*np.mat(locals()
255 ['P_R_' + str(2)])*np.mat(locals()['P_R_'
                + str(3)])*np.mat(locals()['P_R_'
                + str(4)])*np.mat(locals()['P_L_'
                + str(1)])*np.mat(locals()['P_L_'
                + str(2)])*np.mat(locals()['P_L_'
260 + str(3)])*np.mat(locals()['P_L_'
                + str(4)])*np.mat(L2)*np.mat(R1)
                *np.mat(locals()['P_R_' + str(1)])
                *np.mat(locals()['P_R_' + str(2)])
                *np.mat(locals()['P_R_' + str(3)])
265 *np.mat(locals()['P_R_' + str(4)])

B2_lift1234 = np.mat(R4)*np.mat(locals()['P_R_'
                + str(1)])*np.mat(locals()['P_R_' + str(2)])
                *np.mat(locals()['P_R_' + str(3)])*np.mat
                (locals()['P_R_' + str(4)])*np.mat(locals()
270 ['P_L_' + str(1)])*np.mat(locals()['P_L_'
                + str(2)])*np.mat(locals()['P_L_' + str(3)])
                *np.mat(locals()['P_L_' + str(4)])*np.mat(L3)
                *np.mat(R2)*np.mat(locals()['P_R_' + str(1)])

```

```

275     *np.mat(locals()['P_R_' + str(2)])
        *np.mat(locals()['P_R_' + str(3)])
        *np.mat(locals()['P_R_' + str(4)])
        *np.mat(locals()['P_L_' + str(1)])
        *np.mat(locals()['P_L_' + str(2)])
        *np.mat(locals()['P_L_' + str(3)])
280     *np.mat(locals()['P_L_' + str(4)])
        *np.mat(L1)

    file.write('lift four bosons: \n')
    B1_lift1234_eigen1, B1_lift1234_eigen2,
285     B1_lift1234_eigen3, B1_lift1234_eigen4,
    d = calculate_eigenvalues(B1_lift1234)
    B2_lift1234_eigen1, B2_lift1234_eigen2,
    B2_lift1234_eigen3, B2_lift1234_eigen4,
    d = calculate_eigenvalues(B2_lift1234)
290     file.write('eigenvalues for B1:' + ' ' +
        + str(B1_lift1234_eigen1) + ' ' +
        + str(B1_lift1234_eigen2) + ' ' +
        + str(B1_lift1234_eigen3) + ' ' +
        + str(B1_lift1234_eigen4) + "\n")
295     file.write('eigenvalues for B2:' + ' ' +
        + str(B2_lift1234_eigen1) + ' ' +
        + str(B2_lift1234_eigen2) + ' ' +
        + str(B2_lift1234_eigen3) + ' ' +
        + str(B2_lift1234_eigen4) + "\n")
300

# calculation of eigenvalues for a 4 by 4 matrix B
305 def calculate_eigenvalues(B):
    B = sp.Matrix(B)
    # check whether B is diagonal
    diag = 1
    for i in range(4):
310         for j in range(4):
            if i!=j:
                if B[i,j] != 0:
                    diag = 0

315     # if B is diagonal
    if diag == 1:
        eg1 = B[0,0]
        eg2 = B[1,1]
        eg3 = B[2,2]

```

```

320         eg4 = B[3,3]

        # if B is not diagonal
        if diag == 0:
            P, D = B.diagonalize()
325             eg1 = D[0,0]
                eg2 = D[1,1]
                eg3 = D[2,2]
                eg4 = D[3,3]
        return eg1, eg2, eg3, eg4, diag

330 def main():

        # input L matrix
        a = np.loadtxt('adinkra_dict_yangrui.txt')

335         # n is the number of total Adinkras
        for n in range(36864):
            Int_row = 16*n
            file.write('*****
340                 **** Study %d-th Adinkra *****
                    *****\n'%(n+1))
            f2.write('*****
                    ** Study %d-th Adinkra *****
                    *****\n'%(n+1))
345             L1 = a[Int_row:Int_row+4,:]
                L2 = a[Int_row+4:Int_row+8,:]
                L3 = a[Int_row+8:Int_row+12,:]
                L4 = a[Int_row+12:Int_row+16,:]

350             calculation_Bmatrix_eigenvalue(L1, L2, L3, L4)

if __name__ == '__main__':
    main()

```

References

- [1] S. J. Gates, Jr., and L. Rana, “A Theory of Spinning Particles for Large N-extended Supersymmetry (I),” *Phys. Lett.* **B352** (1995) 50; DOI: 10.1016/0370-2693(95)00474-Y, e-Print: arXiv [hep-th:9504025].
- [2] S. J. Gates Jr., and L. Rana, “A Theory of Spinning Particles for Large N-extended Supersymmetry (II),” *ibid. Phys. Lett.* **B369** (1996) 262; DOI: 10.1016/0370-2693(95)01542-6, arXiv [hep-th:9510151].
- [3] M. Faux, and S. J. Gates Jr., “Adinkras: A Graphical technology for supersymmetric representation theory,” *Phys. Rev.* **D71** (2005) 065002, DOI: 10.1103/PhysRevD.71.065002, e-Print: hep-th/0408004; DOI: 10.1103/PhysRevD.71.065002
- [4] C. F. Doran, M. G. Faux, S. J. Gates, Jr., T. Hübsch, K. M. Iga, G. D. Landweber, and R. L. Miller, “Topology Types of Adinkras and the Corresponding Representations of N-Extended Supersymmetry,” UMDEPP-08-010, SUNY-O-667, e-Print: arXiv:0806.0050 [hep-th] (unpublished).
- [5] C. F. Doran, M. G. Faux, S. J. Gates, Jr., T. Hübsch, K. M. Iga, and G. D. Landweber, “Relating Doubly-Even Error-Correcting Codes, Graphs, and Irreducible Representations of N-Extended Supersymmetry,” UMDEPP-07-012 SUNY-O-663, e-Print: arXiv:0806.0051 [hep-th] (unpublished).
- [6] C. F. Doran, M. G. Faux, S. J. Gates, Jr., T. Hübsch, K. M. Iga, G. D. Landweber, and R. L. Miller, “Codes and Supersymmetry in One Dimension,” *Adv. Theor. Math. Phys.* **15** (2011) 6, 1909-1970; DOI: 10.4310/ATMP.2011.v15.n6.a7 e-Print: arXiv:1108.4124 [hep-th].
- [7] C. Doran, K. Iga, J. Kostiuk, G. Landweber, and S. Mendez-Diez, “Geometrization of N-extended 1-dimensional supersymmetry algebras, I,” *Adv. Theor. Math. Phys.* **19** (2015) 1043-1113; DOI: 10.4310/ATMP.2015.v19.n5.a4. e-Print: arXiv:1311.3736 [hep-th].
- [8] C. Doran, K. Iga, J. Kostiuk, G. Landweber, and S. Mendez-Diez, “Geometrization of N-Extended 1-Dimensional Supersymmetry Algebras II,” *Adv. Theor. Math. Phys.* **22** (2018) 565-613; DOI: 10.4310/ATMP.2018.v22.n3.a2, e-Print: arXiv:1610.09983 [hep-th].
- [9] T. F. Banchoff. “Critical Points and Curvature for Embedded Polyhedral Surfaces,” *Am. Math. Monthly*, **70** (5):475-485, May 1970.
- [10] S. J. Gates, Jr., and L. Rana, “Ultramultiplets: A New representation of rigid 2-d, N=8 supersymmetry,” *Phys. Lett.* **B342** (1995) 132-137; DOI: 10.1016/0370-2693(94)01365-J, e-Print: hep-th/9410150.
- [11] B. L. Douglas, S. J. Gates, Jr., and J.-B. Wang, “Automorphism Properties of Adinkras,” Univ of MD Preprint # UMDEPP 10-014, Sep 2010. 34 pp., e-Print: arXiv:1009.1449 [hep-th] (unpublished)
- [12] B. L. Douglas, S. J. Gates, Jr. R. L. Segler, and J.-B. Wang, “Automorphism Properties and Classification of Adinkras,” *Adv. Math. Phys.*, Volume 2015, Article ID 584542, 17 pages, <http://dx.doi.org/10.1155/2015/584542>.

- [13] K. Burghardt and S. J. Gates, Jr., “Adinkra Isomorphisms and Seeing Shapes with Eigenvalues,” Dec 2012. 23 pp., UNIV.-OF-MD-PREPRINT-PP-012-015, e-Print: arXiv:1212.2731 [hep-th] (unpublished).
- [14] M. G. Faux, and, G. D. Landweber, “Spin Holography via Dimensional Enhancement,” Phys. Lett. **B681** (2009) 161-165; DOI: 10.1016/j.physletb.2009.10.014, e-Print: arXiv:0907.4543 [hep-th].
- [15] M. G. Faux, K. M. Iga, and, G. D. Landweber, “Dimensional Enhancement via Supersymmetry,” Adv. Math. Phys. **2011** (2011) 259089; DOI: 10.1155/2011/259089, e-Print: arXiv:0907.3605 [hep-th].
- [16] S. J. Gates, Jr. and T. Hübsch, “On Dimensional Extension of Supersymmetry: From Worldlines to Worldsheets,” Apr 2011. 50 pp. Adv. Theor. Math. Phys. **16** (2012) no.6, 1619-1667; DOI: 10.4310/ATMP.2012.v16.n6.a2; e-Print: arXiv:1104.0722 [hep-th].
- [17] K. Iga, and Y. X. Zhang, “Structural Theory and Classification of 2D Adinkras,” Adv. High Energy Phys. **2016** (2016) 3980613, DOI: 10.1155/2016/3980613 e-Print: arXiv:1508.00491 [hep-th].
- [18] S. J. Gates, Jr., J. Gonzales, B. MacGregor, J. Parker, R. Polo-Sherk, V. G. J. Rodgers and L. Wassink, “4D, $N = 1$ Supersymmetry Genomics (I),” JHEP **0912**, 008 (2009) DOI:10.1088/1126-6708/2009/12/008, [arXiv:0902.3830 [hep-th]].
- [19] S. J. Gates, Jr., K. Iga, L. Kang, V. Korotkikh, and K. Stiffler “Generating all 36,864 Four-Color Adinkras via Signed Permutations and Organizing into ℓ and $\tilde{\ell}$ -Equivalence Classes,” Symmetry **11** (2019) no.1, 120; DOI: 10.3390/sym11010120, e-Print: arXiv:1712.07826 [hep-th].
- [20] T. Kugo, and P. K. Townsend, “Supersymmetry and the Division Algebras,” Nucl. Phys. **B221** (1983) 357-380, DOI: 10.1016/0550-3213(83)90584-9.
- [21] J. C. Baez, and J. Huerta, “Division Algebras and Supersymmetry I” Proc. Symp. Pure Maths. **81** (2010) 65-80; DOI: 10.1090/pspum/081/2681758, e-Print: arXiv:0909.0551 [hep-th].
- [22] J. C. Baez, and J. Huerta, “Division Algebras and Supersymmetry II,” Adv. Theor. Math. Phys. **15** (2011) no.5, 1373-1410; DOI: 10.4310/ATMP.2011.v15.n5.a4, e-Print: arXiv:1003.3436 [hep-th].
- [23] J. Huerta, “Division Algebras and Supersymmetry III” Adv. Theor. Math. Phys. **16** (2012) no.5, 1485-1589; DOI: 10.4310/ATMP.2012.v16.n5.a4, e-Print: arXiv:1109.3574 [hep-th].
- [24] J. Huerta, “Division Algebras and Supersymmetry IV,” Adv. Theor. Math. Phys. **21** (2017) 383-449, DOI: 10.4310/ATMP.2017.v21.n2.a2, e-Print: arXiv:1409.4361 [hep-th].
- [25] D. Z. Freedman, “Gauge Theories of Antisymmetric Tensor Fields,” CALT-68-624.
- [26] M. Sakamoto, “ $N = 1/2$ Supersymmetry in Two-dimensions Phys. Lett. **151B** (1985) 115-118, DOI: 10.1016/0370-2693(85)91396-6.
- [27] R. Brooks, F. Muhammad, S. J. Gates, Jr., “Unidexterous $D=2$ Supersymmetry in Superspace,” Nucl. Phys. **B268** (1986) 599-620, DOI: 10.1016/0550-3213(86)90261-0.
- [28] T. Hübsch, “Weaving Worldsheet Supermultiplets from the Worldlines Within,” Adv. Theor. Math. Phys. **17** (2013) no.5, 903-974, DOI: 10.4310/ATMP.2013.v17.n5.a2, e-Print: arXiv:1104.3135 [hep-th].

- [29] I. Chappell, II, S. J. Gates, Jr, and T. Hübsch, “Adinkra (In)Equivalence From Coxeter Group Representations: A Case Study,” *Int. J. Mod. Phys.* **A29** (2014) 06, 1450029 e-Print: arXiv:1210.0478 [hep-th].
- [30] S. J. Gates, Jr., T. Hübsch, and K. Stiffler, “On Clifford-algebraic Dimensional Extension and SUSY Holography,” *Int. J. Mod. Phys.* **A30** (2015) no.09, 1550042; DOI: 10.1142/S0217751X15500426, e-Print: arXiv:1409.4445 [hep-th].
- [31] Mathew Calkins, D. E. A. Gates, S. J. Gates, Jr, and K. Stiffler, “Adinkras, 0-branes, Holoraumy and the SUSY QFT/QM Correspondence,” *Int. J. Mod. Phys.* **A30** (2015) no.11, 1550050; DOI: 10.1142/S0217751X15500505, e-Print: arXiv:1501.00101 [hep-th].
- [32] S. J. Gates, Jr, T. Grover, M. David Miller-Dickson, B. A. Mondal, A. Oskoui, S. Regmi, E. Ross, and R. Shetty, “A Lorentz Covariant Holoraumy-induced ‘Gadget’ from Minimal Gff-shell 4D, $N=1$ Supermultiplets,” *JHEP* 1511 (2015) 113; DOI: 10.1007/JHEP11(2015)113, e-Print: arXiv:1508.07546 [hep-th].
- [33] S. J. Gates, Jr, Jr., F. Guyton, S. Harmalkar, D. S. Kessler, V. Korotkikh, and V. A. Meszaros, “Adinkras from Ordered Quartets of BC4 Coxeter Group Elements and Regarding 1,358,954,496 Matrix Elements of the Gadget,” *JHEP* 1706 (2017) 006; DOI: 10.1007/JHEP06(2017)006, e-Print: arXiv:1701.00304 [hep-th].
- [34] S. J. Gates, Jr, L. Kang, D. S. Kessler, and V. Korotkikh, “Adinkras from Ordered Quartets of BC4 Coxeter Group Elements and Regarding Another Gadget’s 1,358,954,496 Matrix Elements,” *Int. J. Mod. Phys.* **A33** (2018) no.12, 1850066; DOI: 10.1142/S0217751X18500665, e-Print: arXiv:1802.02890 [hep-th].
- [35] W. Caldwell, A. N. Diaz, I. Friend, S. J. Gates, Jr., S. Harmalkar, T. Lambert-Brown, D. Lay, K. Martirosova, V. A. Meszaros, M. Omokanwaye, S. Rudman, D. Shin, and A. Vershov, “On the Four Dimensional Holoraumy of the 4D, $\mathcal{N} = 1$ Complex Linear Supermultiplet,” *Int. J. Mod. Phys.* **A33** (2018) no.12, 1850072; DOI: 10.1142/S0217751X18500720, e-Print: arXiv:1702.05453 [hep-th].
- [36] M. F. Atiyah, R. Bott, and A. Shapiro “Clifford Modules,” *Topology* **3**, 3-38 (1964).
- [37] H. B. Lawson, Jr. and M. L. Michelsohn, *Spin geometry*, vol. 38 of *Princeton Mathematical Series*. Princeton University Press, Princeton, NJ, 1989.
- [38] A. Pashnev, and F. Toppan, “On the Classification of N-extended Supersymmetric Quantum Mechanical Systems,” *J. Math. Phys.* **42** (2001) 5257-5271, DOI 10.1063/1.1409349, e-Print: arXiv:hep-th/0010135.
- [39] Z. Kuznetsova, M. Rojas, F. Toppan Classification of irreps and invariants of the N-extended Supersymmetric Quantum Mechanics *JHEP* 0603 098, 2006, DOI 10.1088/1126-6708/2006/03/098, e-Print: arXiv:hep-th/0511274;
- [40] Z. Kuznetsova, F. Toppan Refining the classification of the irreps of the 1D N-Extended Supersymmetry *Mod. Phys. Lett.* **A23** 37-51,2008, DOI 10.1142/S0217732308023761, e-Print: arXiv:hep-th/0701225.

- [41] Z.Kuznetsova, F. Toppan Decomposition and Oxidation of the N-Extended Supersymmetric Quantum Mechanics Multiplets Int. J. Mod. Phys. **A23** 3947-3962, 2008, doi 10.1142/S0217751X08042274, e-Print: arXiv:0712.3176.